Essential role of IRF4 and MYC signaling for survival of anaplastic large cell lymphoma

Weilemann A., Grau M., Erdmann T., Merkel O., Sobhiafshar U., Anagnostopoulos I., Hummel M., Siegert A., Hayford C., Madle H., Wollert-Wulf B., Fichtner I., Dörken B., Dirnhofer S., Mathas S., Janz M., Emre N.C.T., Rosenwald A., Ott G., Lenz P., Tzankov A., Lenz G.

Blood
2015 JAN 01 ; 125(1): 124-132
2014 OCT 30 (first published online: accepted manuscript)
doi: 10.1182/blood-2014-08-594507

Publisher: The American Society of Hematology

LYMPHOID NEOPLASIA

Essential role of IRF4 and MYC signaling for survival of anaplastic large cell lymphoma

Andre Weilemann,[1,2,3,4] Michael Grau,[5] Tabea Erdmann,[1,2,3] Olaf Merkel,[6] Ulduz Sobhiafshar,[7] Ioannis Anagnostopoulos,[8] Michael Hummel,[8] Antje Siegert,[9] Claudia Hayford,[2] Hannelore Madle,[1,2,3] Brigitte Wollert-Wulf,[2,10] Iduna Fichtner,[9] Bernd Dörken,[2,10] Stephan Dirnhofer,[11] Stephan Mathas,[2,10] Martin Janz,[2,10] N. C. Tolga Emre,[7] Andreas Rosenwald,[12] German Ott,[13] Peter Lenz,[5] Alexandar Tzankov,[11] and Georg Lenz[1,2,3]

[1]Department of Medicine A, Translational Oncology, Albert-Schweitzer Campus 1, University Hospital Münster, Münster, Germany; [2]Department of Hematology, Oncology, and Tumor Immunology, Charité - Universitätsmedizin Berlin, Berlin, Germany; [3]Cells in Motion Cluster of Excellence, Münster, Germany; [4]Mathematisch-Naturwissenschaftliche Fakultät I, Humboldt University Berlin, Berlin, Germany; [5]Department of Physics, Philipps-University, Marburg, Germany; [6]Department of Experimental Pathology, Medical University Vienna, Wien, Austria; [7]Department of Molecular Biology and Genetics, Boğaziçi University, Bebek, Istanbul, Turkey; [8]Institute of Pathology, Charité - Universitätsmedizin Berlin, Berlin, Germany; [9]Experimental Pharmacology & Oncology Berlin-Buch GmbH, Berlin, Germany; [10]Max-Delbrück-Center for Molecular Medicine, Berlin, Germany; [11]Institute of Pathology, University Hospital, Basel, Switzerland; [12]Department of Pathology, University of Würzburg, Würzburg, Germany; and [13]Department of Clinical Pathology, Robert-Bosch-Krankenhaus, Stuttgart, Germany

Key Points

- IRF4 regulates MYC expression in ALCL.
- ALCL survival depends on IRF4/MYC signaling.

Anaplastic large cell lymphoma (ALCL) is a distinct entity of T-cell lymphoma that can be divided into 2 subtypes based on the presence of translocations involving the *ALK* gene (ALK$^+$ and ALK$^-$ ALCL). The interferon regulatory factor 4 (IRF4) is known to be highly expressed in both ALK$^+$ and ALK$^-$ ALCLs. However, the role of IRF4 in the pathogenesis of these lymphomas remains unclear. Here we show that ALCLs of both subtypes are addicted to IRF4 signaling, as knockdown of IRF4 by RNA interference was toxic to ALCL cell lines in vitro and in ALCL xenograft mouse models in vivo. Gene expression profiling after IRF4 knockdown demonstrated a significant downregulation of a variety of known MYC target genes. Furthermore, our analyses revealed that MYC is a primary target of IRF4, identifying a novel regulatory mechanism of MYC expression and its target gene network in ALCL. MYC, itself, is essential for ALCL survival, as both knockdown of MYC and pharmacologic inhibition of MYC signaling were toxic to ALCL cell lines. Collectively, our results demonstrate that ALCLs are dependent on IRF4 and MYC signaling and that MYC may represent a promising target for future therapies. (*Blood*. 2015;125(1):124-132)

Introduction

ALCL is a distinct subtype of T-cell lymphoma and accounts for 2% to 3% of all malignant lymphoma cases.[1,2] Within the current World Health Organization classification of lymphoid malignancies, 2 different subtypes of ALCL are distinguished based on the presence or absence of translocations involving the anaplastic lymphoma kinase (*ALK*) gene.[3] The vast majority of ALK$^+$ ALCLs are characterized by the t(2;5) (p23;q35) translocation that leads to the fusion of *ALK* to the nucleophosmin (*NPM*) gene resulting in the expression of the *NPM-ALK* chimeric transcript.[4] ALK fusions are associated with activation of the catalytic domain of ALK, leading to constitutive activity of various downstream signaling pathways, such as JAK/STAT or PI3K/AKT.[5-7] Despite these advances in the understanding of the molecular pathogenesis of ALK$^+$ cases, ALCL lymphomagenesis is still not fully understood. In roughly 40% of systemic ALCLs, *ALK* translocations are not detectable, suggesting that not yet identified molecular aberrations may be responsible for ALCL development.[8]

Interferon regulatory factor 4 (IRF4) is a member of the IRF family of transcription factors that consists of 9 members.[9] IRF4 is expressed in most cell types of the immune system and is induced in T-cells by T-cell receptor stimulation.[10] IRF4 binds only weakly to DNA and thus interacts in T-cells with other transcription factors such as JUN and basic leucine zipper transcription factor (ATF-like) to either activate or repress gene expression.[10-12] Different studies reported high IRF4 protein expression measured by immunohistochemistry in the vast majority of primary ALCL cases.[13-15] However, its role in the molecular pathogenesis of these lymphomas remains unknown. To this end, we functionally investigated the role of IRF4 in the biology of ALCL. We detected that ALCLs are addicted to IRF4 by upregulating the oncogenic transcription factor MYC. Knockdown of both IRF4 and MYC induced toxicity in ALCL models, suggesting that the IRF4-MYC circuit may represent a promising molecular target for future therapies.

Material and methods

Cell culture, retroviral constructs, and transduction

The human ALK$^+$ ALCL cell lines, K299, JB6, and SU-DHL-1, the ALK$^-$ ALCL line FE-PD, the Sézary syndrome (SS)-derived cell line HuT 78, the T-acute lymphoblastic leukemia (T-ALL) cell lines Jurkat and KE-37, and the

Submitted August 7, 2014; accepted October 24, 2014. Prepublished online as *Blood* First Edition paper, October 30, 2014; DOI 10.1182/blood-2014-08-594507.

The online version of this article contains a data supplement.

The publication costs of this article were defrayed in part by page charge payment. Therefore, and solely to indicate this fact, this article is hereby marked "advertisement" in accordance with 18 USC section 1734.

multiple myeloma (MM) cell line H929 were cultured in RPMI 1640 with 10% fetal calf serum. DEL (ALK^+ ALCL) and Mac-2A (ALK^- ALCL) cells, as well as the MM cell line U266, were cultured in Iscove modified Dulbecco medium supplemented with 20% human plasma. All cell lines were maintained at 37°C with 5% CO_2.

For efficient retroviral transductions, cell lines were engineered to express the murine ecotropic receptor as previously described.[16,17] Additionally, these cell lines were engineered to express the bacterial tetracycline repressor allowing doxycycline-inducible small hairpin RNA (shRNA) or complementary DNA (cDNA) expression.[16,17] The shRNA-mediated RNA interference and toxicity assays were performed as described.[16,17] In brief, to assess toxicity of the shRNA, retroviruses that coexpress green fluorescent protein (GFP) were used. Flow cytometry was performed 2 days after shRNA transduction to determine the initial GFP-positive proportion of live cells for each shRNA. Subsequently, cells were cultured with doxycycline to induce shRNA expression and sampled over time. The GFP-positive proportion at each time was normalized to that of the negative control shRNA and further normalized to the day 2 fraction. The targeting sequence of *IRF4* shRNAs #1 and #2 were CCGCCATTCCTCTATTCAAGA and GTGCCATTTCTCAGGGAAGTA as described.[18] As a negative control, shRNA, we used a previously described nontoxic shRNA directed against *MSMO1*.[16] Each shRNA experiment was completely reproduced at least 2 times for each cell line. For the shRNA rescue experiment, an *IRF4* cDNA (NM_002460.3) and an *MYC* cDNA (NM_002467.2) were created and the experiment was performed as described.[16] The rescue experiments were reproduced at least 2 times.

Patient samples and immunohistochemistry

Conventional full tissue slides of 82 ALCL samples, 38 ALK^+ and 44 ALK^-, were analyzed within the present study. MYC and IRF4 staining was performed as previously described.[19,20] A cutoff level of ≥30% positive tumor cells was applied to define positivity of a sample as previously described for IRF4 and MYC.[21,22]

Clinical data were available for 14 of 82 patients analyzed. For these patients, treatment consisted of anthracycline-based polychemotherapy with or without radiotherapy.

In vivo xenograft mouse studies

For in vivo testing of the K299 and JB6 xenograft mouse models, 6- to 8-weekold female NOD.Cg-Prkdc severe combined immunodeficiency (SCID) Il2rgtm1Wjl/SzJ (NSG, Jackson Laboratory) mice were used. To induce either *IRF4* shRNA #1 or the nontoxic shRNA directed against *MSMO1*, mice received drinking water supplemented with 1 mg/mL doxycycline (Genaxxon) and 5% sucrose at day 5 of palpable tumors of approximately 30 mm^3. Tumor size was measured 3 times weekly in 2 dimensions using caliper and tumor volume was calculated according to the following formula: $1/2 \times (\text{length} \times \text{width}^2)$. All animal experiments were conducted in accordance with the United Kingdom Co-ordinating Committee on Cancer Research guidelines for the welfare of animals and the German animal protection law. Detailed protocols are available in the supplemental Material and Methods on the *Blood* web site.

Gene expression profiling

Gene expression profiling was performed as previously described.[23] Detailed protocols are available in the supplemental Material and Methods.

Quantitative PCR

Quantitative polymerase chain reaction (PCR) was performed as previously described using predesigned assays (Applied Biosystems).[16] *IRF4/MYC* messenger RNA (mRNA) expression was normalized to the expression of *GAPDH*.

Western blotting

Protocols are available in the supplemental Material and Methods on the *Blood* Web site.

Chromatin immunoprecipitation

Detailed protocols are available in the supplemental Material and Methods. Previously described primer pairs were used for chromatin immunoprecipitation (ChIP) real-time PCR to investigate IRF4 binding in the *MYC* promoter and in a control locus.[18,24,25] The applied primer pairs are summarized in supplemental Table 1.

In vitro viability assay and inhibitor studies

Cell viability of ALCL cell lines and U266 cells after JQ1 (Tocris Bioscience) and 10058-F4 (Sigma-Aldrich) inhibitor treatment was assessed using the CellTiter-Glo Luminescent Cell Viability Assay (Promega) after 3 and 4 days of incubation, respectively, as described.[16] Each experiment was reproduced 3 times for each cell line. Inhibitor studies using the ALK inhibitor crizotinib were performed methodically as described.[16]

Results

IRF4 is highly expressed in ALCL

Previous work suggested that IRF4 is expressed in the majority of primary ALCL cases.[13-15] To confirm these results, we assessed IRF4 protein expression in 82 primary ALCL patient samples by immunohistochemistry. Of these, 38 samples were ALK^+, whereas 44 were ALK^-. Overall, 75 of 82 (91%) cases stained positive for IRF4 (Figure 1A). Forty-three of 44 (98%) ALK^- ALCLs expressed IRF4, whereas 32 of 38 (84%) ALK^+ ALCLs had detectable IRF4 expression levels ($P = .045$; IRF4 expression in ALK^- vs ALK^+ ALCLs; 2-tailed Fisher's exact test).

IRF4-positive and IRF4-negative cases could not be distinguished morphologically or pathologically. For a total of 14 patients, we were able to obtain clinical follow-up data. The median follow-up for these 14 patients was 49 months (range 6-288 months). In this cohort, 7 events occurred during follow-up (3 patients relapsed and 4 patients died [2 due to treatment-resistant progressive disease and 2 due to secondary malignancies]). Expression of none of the investigated immunohistochemical markers (IRF4 [$P = .78$] and MYC [$P = .37$] see below) were associated with differences in survival, albeit given the small sample size, one has to be very cautious in drawing definitive conclusions from these analyses.

Next, we analyzed whether established ALCL cell lines represent adequate models for functional analyses of IRF4. To this end, we determined *IRF4* mRNA expression levels by quantitative PCR in 6 ALCL cell lines (including the 4 ALK^+ cell lines K299, JB6, DEL, SU-DHL-1, and the 2 ALK^- cell lines, FE-PD and Mac-2A). The MM cell line H929 served as a positive control, whereas the SS-derived cell line HuT 78 and 2 T-ALL cell lines (Jurkat and KE-37) were used as negative controls. All ALCL cell lines expressed higher *IRF4* mRNA levels compared with the negative control lines and similar or higher levels compared with the levels detected in H929 cells (Figure 1B). These data were confirmed when IRF4 protein expression was investigated by western blotting. Five of 6 ALCL cell lines had high IRF4 expression levels (K299, JB6, DEL, FE-PD, and Mac-2A). Only SU-DHL-1 cells were characterized by low IRF4 expression (Figure 1C). In contrast, HuT 78 cells had low IRF4 expression levels, whereas Jurkat and KE-37 did not have any detectable IRF4 levels. Collectively, these data suggest that ALCL cell lines represent adequate models for functional analyses of IRF4.

Downregulation of IRF4 is toxic to ALCL in vitro and in vivo

To elucidate the functional significance of IRF4 in ALCL, we knocked down its expression using 2 previously described specific shRNAs.[18]

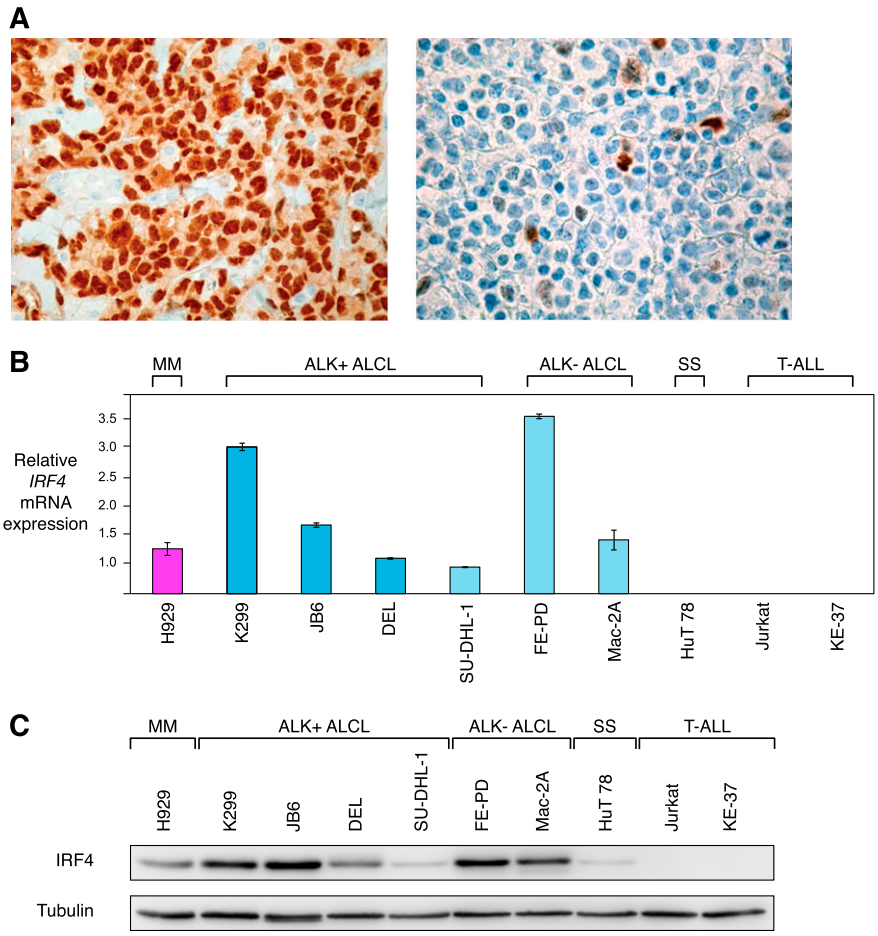

Figure 1. IRF4 is highly expressed in ALCL. (A) Immunohistochemical IRF4 staining of an IRF4-positive ALCL case (left) with internal negative controls (tumor-infiltrating macrophages and endothelia), and an IRF4-negative ALCL case (right) (original magnification ×320). (B) *IRF4* mRNA is highly expressed in ALCL compared with the SS cell line HuT 78 and T-ALL cell lines as measured by quantitative PCR. *IRF4* mRNA levels were normalized to expression of *GAPDH*. Error bars indicate standard deviation. (C) Western blot analysis of IRF4 expression in MM, ALCL, SS, and T-ALL cell lines. Five of 6 ALCL cell lines have high IRF4 protein expression.

Both *IRF4* shRNAs significantly decreased IRF4 expression on mRNA level after 48 hours of shRNA induction and on protein level after 96 hours (Figure 2A-B). Transduction of these shRNAs induced toxicity in the positive MM control cell line H929, as described,[18] and in ALCL cell lines expressing high levels of IRF4 (K299, JB6, DEL, FE-PD, and Mac-2A) (Figure 2C), whereas viability of SU-DHL-1 cells that are characterized by low IRF4 expression (Figure 1C) was not affected, despite significant IRF4 knockdown (Figure 2C; supplemental Figure 1A). Likewise, IRF4 downregulation did not affect survival of SS (HuT 78) or T-ALL cell lines (Jurkat and KE-37) that were used as negative controls (Figure 2C). A previously described, nontoxic shRNA directed against *MSMO1*[16] that we used as a negative control, did not induce any toxicity in our panel of cell lines (supplemental Figure 1B).

To demonstrate that *IRF4* shRNA-mediated toxicity was specifically caused by IRF4 knockdown, we performed a rescue experiment by transducing K299, FE-PD, and Mac-2A cells with a vector that carries the *IRF4* coding region, which is not targeted by *IRF4* shRNA #2. Indeed, exogenous IRF4 expression rescued all ALCL cells from shRNA-mediated toxicity, indicating the specificity of our approach (Figure 2D).

We next determined if IRF4 dependency translates into an in vivo setting. To this end, we created ALCL xenograft mouse models using K299 and JB6 cells that were transduced with vectors that encode either *IRF4* shRNA #1 or a control shRNA. Correspondingly, shRNA-mediated IRF4 knockdown was detectable in tumor samples from *IRF4* shRNA-transduced cells compared with control shRNA transduced tumor samples (Figure 2E). In both JB6 and K299 models, IRF4 knockdown significantly impaired lymphoma growth over 14 days compared with ALCL cells transduced with the previously described nontoxic, control shRNA directed against *MSMO1*[16] ($P = .0007$ for K299, *IRF4* shRNA vs control shRNA; $P = .03$ for JB6, *IRF4* shRNA vs control shRNA; paired Student's *t* test) (Figure 2F), indicating that IRF4 promotes ALCL lymphoma growth. Collectively, our results indicate that ALCLs are dependent on the function of the transcription factor IRF4. Furthermore, this addiction is detectable in both ALK^+ and ALK^- ALCLs, indicating that the same pathways can be used by these 2 lymphoma subtypes.

NPM-ALK signaling upregulates IRF4 in ALCL

Previous work suggested that NPM-ALK signaling promotes IRF4 expression.[26] To investigate if NPM-ALK signaling contributes to upregulated IRF4 expression in our panel of ALCL cell lines, we used the specific ALK inhibitor crizotinib. Treatment of ALK^+ (K299 and JB6) and ALK^- (FE-PD and Mac-2A) cells with 150 nM crizotinib for 24 hours significantly downregulated IRF4 expression in the 2 ALK^+ cell lines, whereas the IRF4 levels in FE-PD and Mac2A cells were unaffected (Figure 2G). These results suggest that NPM-ALK signaling contributes to IRF4 upregulation in ALK^+ ALCL.

IRF4 promotes MYC expression in ALCL

To investigate which biologic processes are regulated by IRF4 in ALCL, we profiled gene expression changes after 24, 48, 72, and 96 hours after IRF4 knockdown in the 2 ALK^+ cell lines K299, and

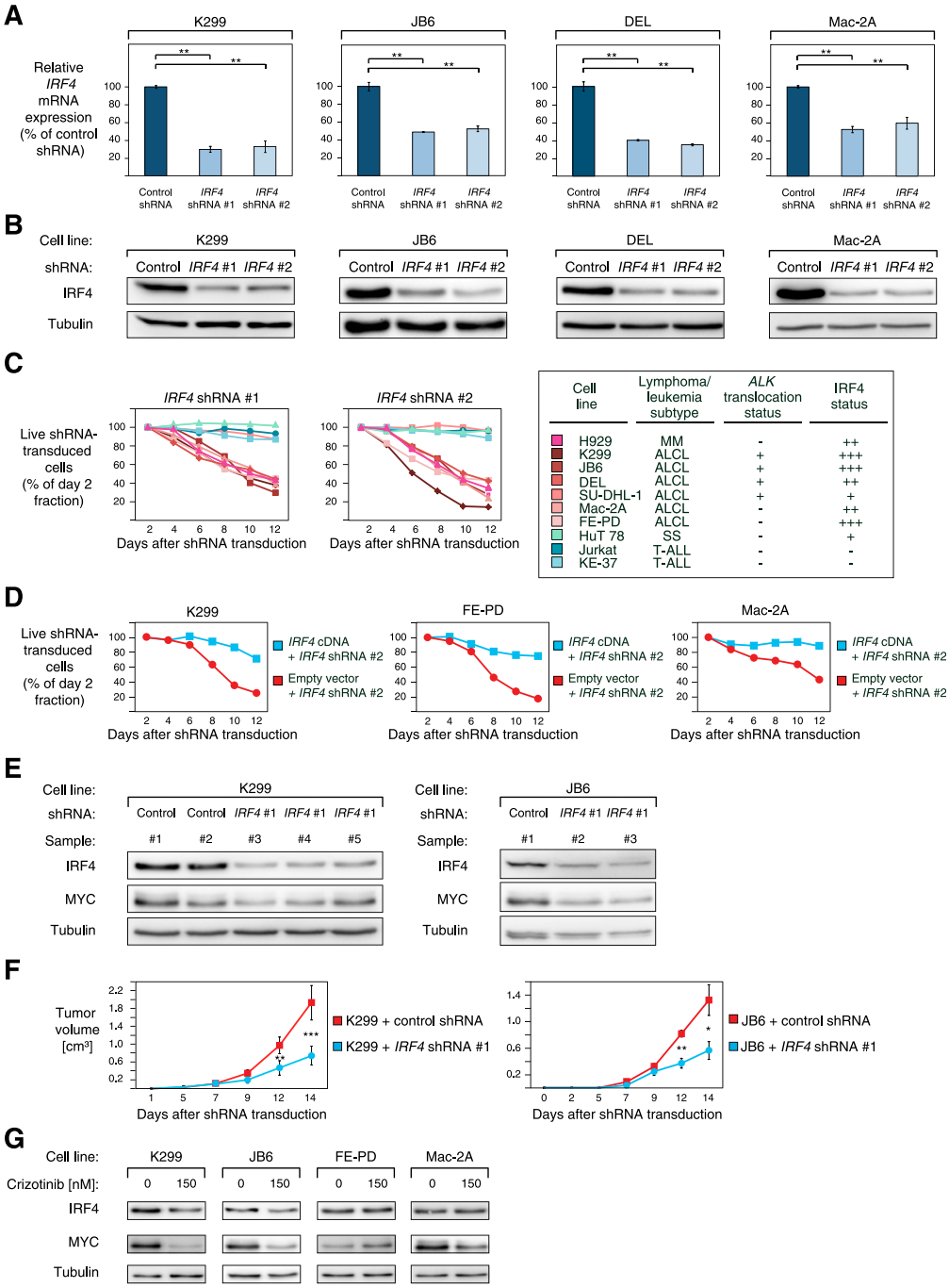

Figure 2. ALCLs are addicted to IRF4. (A) *IRF4* shRNA #1 and #2 downregulate *IRF4* mRNA in K299, JB6, DEL, and Mac-2A cells 48 hours after shRNA induction measured by quantitative PCR. *IRF4* mRNA levels were normalized to expression of *GAPDH*. Error bars indicate standard deviation. (B) *IRF4* shRNA #1 and #2 downregulate IRF4 protein in K299, JB6, DEL, and Mac-2A cells 96 hours after shRNA induction measured by western blotting. (C) IRF4 knockdown by two independent shRNAs is toxic to IRF4-positive ALCL cell lines. In contrast, the IRF4 low expressing ALCL cell line SU-DHL-1, the SS cell line HuT 78, and IRF4-negative T-ALL cell lines are not affected by IRF4 downregulation. Representative results from at least 2 independent replicates are shown. Baseline expression of IRF4 in the investigated cell lines is indicated based on western blotting (Figure 1C) and the *ALK* translocation status is indicated. (D) Exogenous expression of *IRF4* cDNA rescues K299, FE-PD, and Mac-2A cells from *IRF4* shRNA-induced toxicity. Representative results from 3 independent replicates are shown. (E) IRF4 and MYC knockdown is detectable by western blotting in mouse xenograft (K299 and JB6) tumor biopsies from cells transduced with *IRF4* shRNA #1 compared with control shRNA transduced cells (shRNA directed against *MSMO1*). (F) Tumor growth curve of K299 and JB6 xenograft mouse models that inducibly express *IRF4* shRNA #1 (blue) or a control shRNA directed against *MSMO1* (red). IRF4 knockdown significantly reduced in vivo tumor growth ($P = .0007$ for K299, *IRF4* shRNA vs control shRNA; $P = .03$ for JB6, *IRF4* shRNA vs control shRNA; paired Student *t* test). Error bars indicate standard error of the mean. (G) Treatment of ALK$^+$ (K299 and JB6) and ALK$^-$ (FE-PD and Mac-2A) ALCL cell lines with 150 nM crizotinib for 24 hours leads to IRF4 and MYC downregulation as measured by western blotting. *$P < .05$, **$P < .01$, ***$P < .001$.

DEL and in the ALK$^-$ cell line FE-PD. To identify IRF4 regulated genes in both ALCL subtypes, we created a common gene expression signature consisting of genes that were consistently downregulated or upregulated across all time points in all 3 cell lines (Figure 3A; supplemental Table 2). Thus, we identified 115 genes that were significantly downregulated and 211 genes that were significantly upregulated ($P < .0025$) after IRF4 silencing (Figure 3A; supplemental Table 2).

IRF4 knockdown in ALK$^+$ and ALK$^-$ ALCLs affected expression of various genes known to be involved in critical cellular processes such as cell cycle control (eg, *CDKN1A*, *CDKN2D*, *E2F6*), cell proliferation (eg, *BAG2*, *CELF1*, *TYRO3*), or DNA repair (eg, *ATM*, *LIG3*) (Figure 3A). In addition, we identified several known MYC target genes (eg, *GNL3*, *MINA*) that were deregulated after IRF4 knockdown. Moreover, *MYC* mRNA itself was significantly repressed by IRF4 knockdown ($P = .01$; paired *t* test), suggesting that IRF4 silencing leads to suppression of MYC and its target gene network. To test this hypothesis and obtain a better understanding of the gene expression changes in an unbiased manner, we performed a gene set enrichment analysis using previously described gene expression signatures.[27,28] This analysis revealed that the most significantly downregulated gene signature was a previously described MYC target gene set ("Myc_overexpression_1.5×_up"; $P < .001$; false discovery rate [FDR] = 0.001) (Figure 3B; supplemental Figure 2A and supplemental Table 3). In addition, 2 other independent MYC target gene sets were significantly enriched with downregulated genes, indicating that MYC activity is inhibited by IRF4 downregulation ("Myc_RNAi_OCILy3"; $P < .001$; FDR = 0.001 and "Myc_ChIP_PET_Expr_Up"; $P < .001$; FDR = 0.001) (supplemental Table 3). To further confirm these results, we obtained several MYC target gene signatures from the Molecular Signatures Database.[29] Indeed, all 5 MYC signatures were enriched with downregulated genes (supplemental Figure 2B; supplemental Table 4). Thus, our data indicate that IRF4 regulates MYC and its target gene network in both ALK$^+$ and ALK$^-$ ALCL.

Besides MYC target gene sets, several signatures involved in critical cellular processes such as cell proliferation, HIF1A signaling, and Notch signaling were significantly downregulated after IRF4 silencing, indicating a potentially important role of IRF4 in regulating these processes and pathways (supplemental Table 3).

To confirm the gene expression data that MYC expression is controlled by IRF4 in ALCL cells, we determined MYC mRNA and protein expression levels after *IRF4* shRNA-mediated knockdown. Real-time PCR confirmed that *MYC* mRNA is significantly downregulated in ALK$^+$ (K299 and JB6) and ALK$^-$ (FE-PD) ALCL cell lines 48 hours after IRF4 knockdown (Figure 3C). Next, we investigated if IRF4 silencing represses MYC protein levels. Indeed, western blotting corroborated that IRF4 knockdown results in MYC protein downregulation in K299, JB6, and FE-PD cells 48 hours after shRNA induction (Figure 3D). These data were confirmed in vivo in our xenograft models, as MYC protein knockdown was detectable in tumors derived from cells transduced with *IRF4* shRNA #1 compared with cells transduced with a control shRNA (Figure 2E). At last, we determined MYC protein levels 24 hours after crizotinib treatment using western blot analysis. Crizotinib treatment significantly downregulated both IRF4 and MYC protein expression, supporting our data of an IRF4-MYC circuit (Figure 2G).

To investigate whether MYC is a primary or secondary IRF4 target, we performed conventional IRF4 ChIP of the *MYC* promoter in DEL (ALK$^+$) and FE-PD (ALK$^-$) cells. In both cell lines, we detected IRF4 binding in the *MYC* promoter using previously described primer pairs,[24] involving the regions −0.4 to +0.3 kb with respect to the *MYC* transcriptional start site (Figure 3E). Thus, our data indicate that MYC is a primary IRF4 target in ALK$^+$ and ALK$^-$ ALCL cells and that IRF4, therefore, directly controls the MYC-driven gene expression network in these lymphomas.

MYC is critical for ALCL survival and may represent a novel target for ALCL therapy

As our analyses identified MYC as one of the predominant IRF4 target genes, we investigated its role in mediating ALCL cell survival. First, we determined MYC expression in our panel of ALCL cell lines and in our cohort of primary ALCL samples. All ALCL cell lines expressed MYC levels as determined by western blotting (Figure 4A), whereas 69 of 82 (84%) primary ALCL samples were MYC-positive measured by immunohistochemistry (Figure 4B). MYC expression was irrespective of the ALK status. Thirty-eight of 44 (86%) primary ALK$^-$ ALCLs expressed MYC, whereas 31 of 38 (82%) ALK$^+$ ALCLs had detectable MYC expression ($P = .76$; MYC expression in ALK$^+$ vs ALK$^-$ ALCLs; 2-tailed Fisher's exact test). In 67 of 82 (82%) samples, both IRF4 and MYC were coexpressed and thus IRF4-positive samples were more frequently MYC positive compared with IRF4 negative cases ($P = 8.3 \times 10^{-4}$; Fisher's exact test).

To functionally analyze the role of MYC for ALCL survival, we knocked down its expression using 2 different specific shRNAs that mediate significant MYC downregulation 96 hours after shRNA induction (Figure 4C). MYC silencing induced cytotoxicity in all ALCL cell lines, confirming that MYC plays a pivotal role for ALCL survival (Figure 4D). As expected, expression of an *MYC* cDNA rescued ALCL cells from MYC knockdown-induced toxicity, confirming the specificity of our shRNA approach (Figure 4E).

To evaluate the degree to which MYC downregulation contributes to IRF4 knockdown-induced toxicity, we performed a rescue experiment in which we introduced an *MYC* cDNA or an empty vector in *IRF4* #1 and #2 shRNA-transduced DEL, JB6, and FE-PD cells. We detected a complete MYC-induced rescue in DEL cells indicating that MYC knockdown significantly contributes to the lethal effect of IRF4 downregulation in these cells. In contrast, in JB6 and FE-PD cells, no *MYC* cDNA-induced rescue was detectable (Figure 4F), indicating that deregulation of additional signaling pathways contributes to the IRF4 knockdown-induced toxicity in these cells.

Finally, we tested whether the addiction to MYC signaling can be exploited therapeutically. To this end, we treated ALCL cell lines with the BET family inhibitor JQ1 that downregulates MYC expression, and we determined cell viability after 3 days of incubation.[30,31] The MM cell line U266 that does not express MYC (Figure 4A), but MYCL,[32] was used as a negative control. JQ1 significantly reduced cell viability of all ALCL cell lines irrespective of their *ALK* translocation status, whereas viability of U266 was not affected (Figure 4G). These data were supported when we treated our ALCL cell line panel and U266 with the small molecule inhibitor 10058-F4 that inhibits MYC-MAX heterodimerization.[33] Viability of most ALCL cell lines was strongly affected by MYC-MAX inhibition compared with the control cell line (supplemental Figure 3). Collectively, our data indicate an important role of MYC in maintaining ALCL survival that can be blocked pharmacologically, suggesting that MYC inhibition may represent a novel therapeutic approach for ALCL patients.

Discussion

Within the present study, we have identified an unexpected role of IRF4 in the biology of ALK$^+$ and ALK$^-$ ALCLs. Our data demonstrate that both subtypes of ALCL are addicted to the IRF4 gene expression network, as IRF4 knockdown induced toxicity in ALCL models both in vitro and in vivo. The molecular mechanisms leading to IRF4 upregulation in ALCL remain not to be completely understood. Translocations involving *IRF4* have been described in peripheral T-cell lymphoma such as cutaneous ALCL, but are very rare in systemic ALCL.[15] The NPM-ALK chimeric protein and IL-2

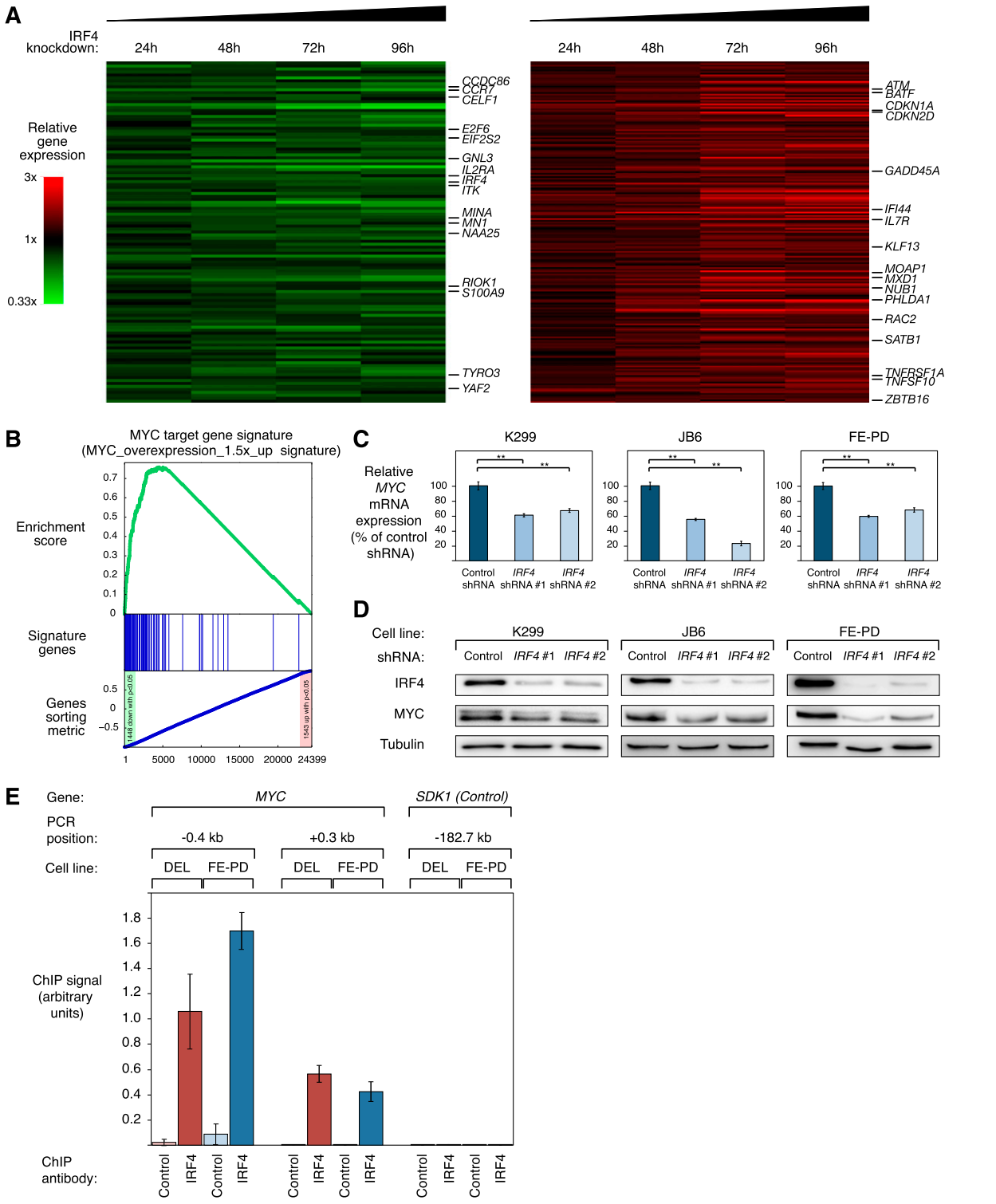

Figure 3. IRF4 downregulation suppresses the gene expression network of MYC in ALCL. (A) Gene expression profiling after IRF4 knockdown in K299, DEL, and FE-PD cells. Changes of gene expression were profiled at the indicated time points after induction of *IRF4* shRNA #1. Gene expression changes are depicted according to the color scale shown. Genes that are involved in critical biological processes are highlighted. (B) Gene set enrichment analysis of a previously described MYC gene expression signature. The MYC signature is significantly enriched with genes that are downregulated after IRF4 knockdown. (C) *IRF4* shRNA #1 and #2 downregulate *MYC* mRNA in K299, JB6, and FE-PD cells 48 hours after shRNA induction as measured by quantitative PCR. *MYC* mRNA levels were normalized to expression of *GAPDH*. Error bars indicate the standard deviation. (D) *IRF4* shRNA #1 and #2 downregulate MYC protein in K299, JB6, and FE-PD cells 48 hours after shRNA induction as measured by western blotting. (E) Chromatin immunoprecipitation quantitative PCR analysis of IRF4 binding in the *MYC* promoter and at a control locus in DEL (ALK^+) and FE-PD (ALK^-) cells. The control locus is a region on chromosome 7, used as a negative control for IRF4 binding, due to the lack of observable IRF4 binding in previous studies.[24,25] Error bars depict standard error of the mean. $^{**}P < .01$.

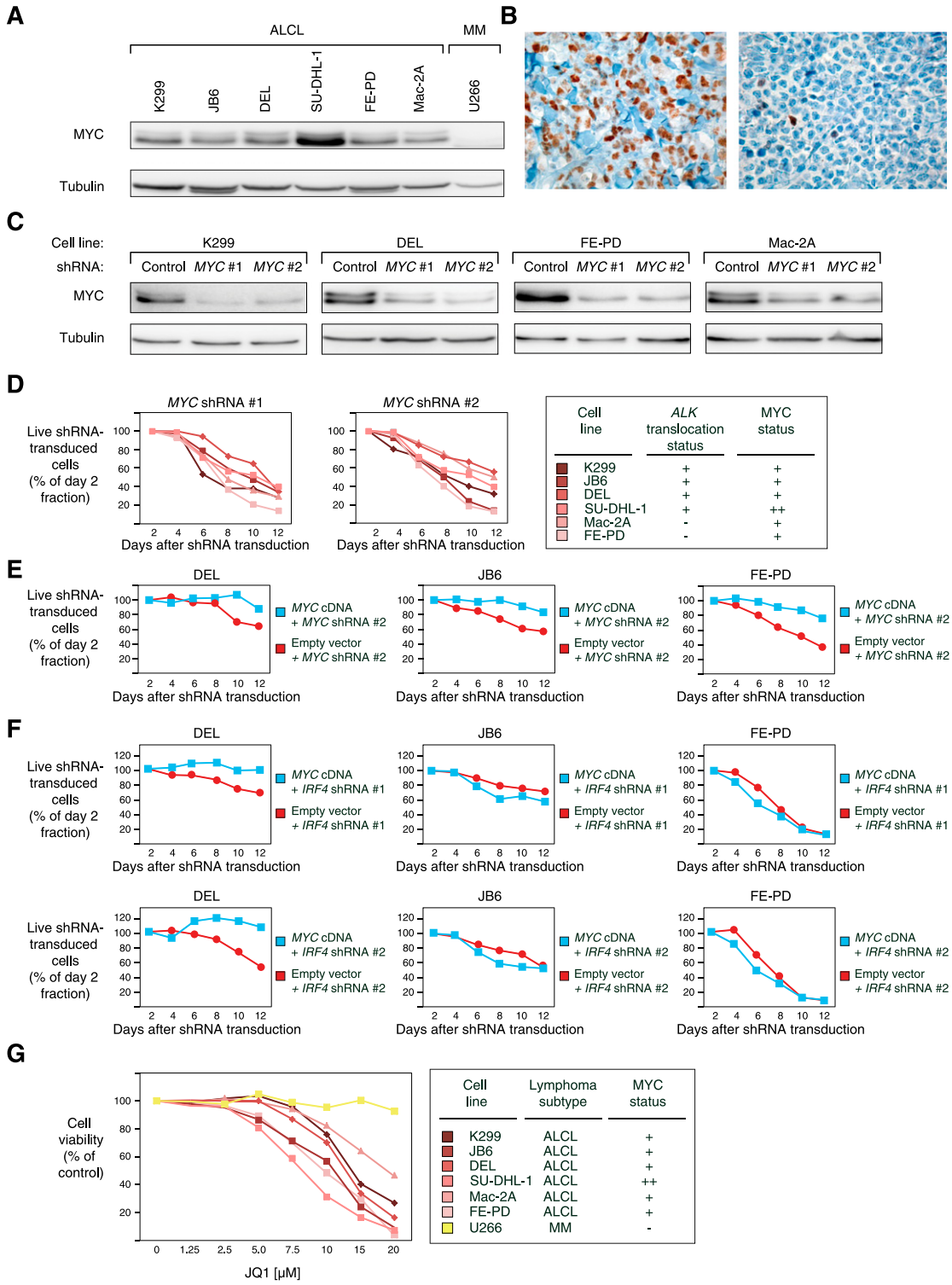

Figure 4. ALCLs depend in their survival on MYC signaling. (A) Western blot analysis of MYC expression in 6 ALCL cell lines and in the MM cell line U266. All ALCL cell lines have detectable MYC expression compared with the negative control U266. (B) Immunohistochemical MYC staining of an MYC-positive ALCL case (left) and an MYC-negative ALCL case (right) (original magnification ×320). (C) *MYC* shRNA #1 and #2 significantly downregulate MYC protein 96 hours after induction measured by western blotting in K299, DEL, FE-PD, and Mac-2A cells. (D) shRNA-mediated MYC knockdown is toxic to ALCL cell lines. Baseline expression of MYC in the investigated cell lines based on western blotting (seen in panel A) and the *ALK* translocation status are indicated. Representative results are shown. (E) Expression of an *MYC* cDNA rescues DEL, JB6, and FE-PD cells, transduced with *MYC* shRNA #2 (targeting the 3′UTR [untranslated region] of *MYC*) from toxicity. Representative results from 2 independent replicates are shown. (F) Expression of an *MYC* cDNA rescues DEL cells, transduced with *IRF4* shRNA #1 and #2 from toxicity. In contrast, JB6 and FE-PD cells are not rescued from shRNA-induced toxicity. Representative results from at least 2 independent replicates are shown. (G) ALCL cell lines are sensitive to MYC inhibition using the BET family inhibitor JQ1 after 3 days of incubation. Viability of the negative control cell line U266 is not affected by JQ1. Baseline expression of MYC in the investigated cell lines based on western blotting (seen in panel A) is indicated. Representative results of 3 replicates are shown.

signaling have been shown to upregulate IRF4 protein by activating the transcription factors STAT3 and STAT5 in T-cell lymphoma cells.[26] The role of NPM-ALK signaling in mediating IRF4 expression was confirmed in our study, as treatment with the ALK inhibitor crizotinib downregulated IRF4 expression in ALK^+ ALCL cell lines. However, as both ALK^+ and ALK^- ALCLs express IRF4, potentially other molecular mechanisms promote IRF4 expression in these lymphomas. In the activated B-cell–like (ABC) subtype of diffuse large B-cell lymphoma (DLBCL) it was recently shown that IRF4 is a target gene of the oncogenic nuclear factor-κB (NF-κB) signaling pathway.[34,35] In ALCL, previous studies showed that the NPM-ALK fusion protein suppresses NF-κB activation in ALK^+ ALCL.[36] However, it is possible that in ALK^- ALCLs, NF-κB signaling might be involved in IRF4 regulation, and this should be addressed in future work.

Our gene expression analyses revealed that IRF4 knockdown affects a number of critical cellular processes such as proliferation, apoptosis, and DNA damage, and potentially oncogenic signaling pathways such as Notch indicating a central role of IRF4 in the molecular pathogenesis of ALCL. The predominant primary IRF4 target that emerged from our analyses is the oncogenic transcription factor MYC. MYC is aberrantly expressed in a variety of different forms of cancer and plays an important role in the biology of various lymphoma subtypes such as Burkitt lymphoma or DLBCL.[37] MYC regulates roughly 15% of all genes in the human genome and has known activating and repressing functions on its target genes. It is involved in the regulation of cell cycle control, cell growth, protein synthesis, angiogenesis, and apoptosis.[37] Previous work by Raetz et al[38] suggested that MYC is a downstream target of ALK and thus it is predominantly expressed in ALK^+ ALCLs. In this study, all ALK^- ALCLs did not express MYC protein as measured by immunohistochemistry.[38] However, our results indicate that IRF4 upregulates MYC in both ALK^+ and ALK^- ALCLs. Accordingly, we could not confirm a difference in MYC expression in ALK^+ and ALK^- ALCLs, as MYC was detectable in cell lines and in primary patient samples of both subtypes. The discrepant immunohistochemistry results may be caused by the use of different antibodies and differences in the staining techniques.[38]

Previous work identified MYC as a direct transcriptional target of IRF4 in MM cells.[18] In contrast, IRF4, which is also involved in the biology of ABC DLBCL, does not bind to the *MYC* promoter in these lymphomas.[25] Given that IRF4 upregulates MYC expression in ALCL as indicated by our results, it seems conceivable that IRF4 regulates specific target genes and gene expression networks in a context-dependent manner. One possible explanation is that IRF4, which only binds weakly to DNA by itself, interacts with different DNA binding partners in these different hematologic malignancies. However, additional analyses in the future are required to decipher these specific IRF4 functions.

IRF4 and MYC expression measured by immunohistochemistry were significantly associated with each other and both proteins were coexpressed in 82% of the samples. However, in some cases, IRF4 and MYC expression did not correlate, potentially indicating that additional molecular mechanisms regulate MYC expression in ALCL. Translocations affecting *MYC* are infrequent in these lymphomas and seem to be associated with an aggressive clinical course.[39-41] In contrast, a recent study using array comparative genomic hybridization on primary ALCL samples reported recurrent *MYC* gains.[42] In addition, other MYC upregulating mechanisms may be used by ALCL.

Despite the evident role of IRF4 in mediating MYC expression in ALCL, we detected a MYC-induced rescue of IRF4-induced toxicity in only 1 of 3 ALCL cell lines. Potentially, these data can be explained by different mechanisms. It is possible that the survival of the 2 cell lines that were not rescued by MYC depend on additional signaling pathways that are deregulated by IRF4 knockdown such as HIF1A or Notch. Alternatively, we cannot completely rule out technical reasons such as inadequate MYC expression in these cells.

Finally, we evaluated if addiction to MYC signaling can be exploited therapeutically in ALCL. Despite improvements in therapy, there is still a significant fraction of patients diagnosed with ALCL who succumb to their disease.[43] Two different MYC inhibitors induced cytotoxicity in all ALK^+ and ALK^- ALCL cell line models. These data suggest that MYC inhibition may offer a promising target and a novel therapeutic strategy to overcome therapy resistance in patients diagnosed with ALCL, irrespective of their ALK status.

Acknowledgments

This work was supported by research grants from the Deutsche Krebshilfe and the Swiss National Science Foundation (Sinergia grant) (G.L.); the Deutsche Forschungsgemeinschaft, DFG EXC 1003 Cells in Motion - Cluster of Excellence, Münster, Germany, and a Doctoral Scholarship from the Philipps-University Marburg (M.G.).

Authorship

Contribution: A.W., U.S., I.A., M.H., A.S., C.H., H.M., and B.W.-W. performed experiments; A.W. and G.L. designed research; A.W. and G.L. wrote the manuscript; M.G. performed bioinformatic and biophysical analyses; T.E., U.S., I.A., M.H., and A.S. analyzed experiments; and O.M., I.F., B.D., S.D., S.M., M.J., N.C.T.E., A.R., G.O., P.L., A.T., and G.L. analyzed data.

Conflict-of -interest disclosure: The authors declare no competing financial interest.

Correspondence: Georg Lenz, Medical Department A, University Hospital Münster, Translational Oncology, Albert-Schweitzer Campus 1, 48149 Münster, Germany; e-mail: georg.lenz@ukmuenster.de.

References

1. Piccaluga PP, Gazzola A, Mannu C, et al. Pathobiology of anaplastic large cell lymphoma. *Adv Hematol.* 2010;345053 [published online ahead of print February 6, 2011]. *Blood.* doi: 10.1155/2010/345053.
2. Fornari A, Piva R, Chiarle R, Novero D, Inghirami G. Anaplastic large cell lymphoma: one or more entities among T-cell lymphoma? *Hematol Oncol.* 2009;27(4):161-170.
3. Swerdlow SH, Campo E, Harris NL, et al. WHO Classification of Tumours of Haematopoietic and Lymphoid Tissues. Lyon, France: IARC Press; 2008.
4. Morris SW, Kirstein MN, Valentine MB, et al. Fusion of a kinase gene, ALK, to a nucleolar protein gene, NPM, in non-Hodgkin's lymphoma. *Science.* 1994;263(5151): 1281-1284.
5. Chiarle R, Voena C, Ambrogio C, Piva R, Inghirami G. The anaplastic lymphoma kinase in the pathogenesis of cancer. *Nat Rev Cancer.* 2008;8(1):11-23.
6. Bai RY, Ouyang T, Miething C, Morris SW, Peschel C, Duyster J. Nucleophosmin-anaplastic lymphoma kinase associated with anaplastic large-cell lymphoma activates the phosphatidylinositol 3-kinase/Akt antiapoptotic

signaling pathway. *Blood.* 2000;96(13):4319-4327.

7. Zamo A, Chiarle R, Piva R, et al. Anaplastic lymphoma kinase (ALK) activates Stat3 and protects hematopoietic cells from cell death. *Oncogene.* 2002;21(7):1038-1047.
8. Stein H, Foss HD, Dürkop H, et al. CD30(+) anaplastic large cell lymphoma: a review of its histopathologic, genetic, and clinical features. *Blood.* 2000;96(12):3681-3695.
9. Huber M, Lohoff M. IRF4 at the crossroads of effector T-cell fate decision. *Eur J Immunol.* 2014;44(7):1886-1895.
10. Li P, Spolski R, Liao W, et al. BATF-JUN is critical for IRF4-mediated transcription in T cells. *Nature.* 2012;490(7421):543-546.
11. Tussiwand R, Lee WL, Murphy TL, et al. Compensatory dendritic cell development mediated by BATF-IRF interactions. *Nature.* 2012;490(7421):502-507.
12. Glasmacher E, Agrawal S, Chang AB, et al. A genomic regulatory element that directs assembly and function of immune-specific AP-1-IRF complexes. *Science.* 2012;338(6109):975-980.
13. Falini B, Fizzotti M, Pucciarini A, et al. A monoclonal antibody (MUM1p) detects expression of the MUM1/IRF4 protein in a subset of germinal center B cells, plasma cells, and activated T cells. *Blood.* 2000;95(6):2084-2092.
14. Tsuboi K, Iida S, Inagaki H, et al. MUM1/IRF4 expression as a frequent event in mature lymphoid malignancies. *Leukemia.* 2000;14(3):449-456.
15. Feldman AL, Law M, Remstein ED, et al. Recurrent translocations involving the IRF4 oncogene locus in peripheral T-cell lymphomas. *Leukemia.* 2009;23(3):574-580.
16. Wenzel SS, Grau M, Mavis C, et al. MCL1 is deregulated in subgroups of diffuse large B-cell lymphoma. *Leukemia.* 2013;27(6):1381-1390.
17. Ngo VN, Davis RE, Lamy L, et al. A loss-of-function RNA interference screen for molecular targets in cancer. *Nature.* 2006;441(7089):106-110.
18. Shaffer AL, Emre NC, Lamy L, et al. IRF4 addiction in multiple myeloma. *Nature.* 2008;454(7201):226-231.
19. Tzankov A, Xu-Monette ZY, Gerhard M, et al. Rearrangements of MYC gene facilitate risk stratification in diffuse large B-cell lymphoma patients treated with rituximab-CHOP. *Mod Pathol.* 2014;27(7):958-971.
20. Hoeller S, Zihler D, Zlobec I, et al. BOB.1, CD79a and cyclin E are the most appropriate markers to discriminate classical Hodgkin's lymphoma from primary mediastinal large B-cell lymphoma. *Histopathology.* 2010;56(2):217-228.
21. Hans CP, Weisenburger DD, Greiner TC, et al. Confirmation of the molecular classification of diffuse large B-cell lymphoma by immunohistochemistry using a tissue microarray. *Blood.* 2004;103(1):275-282.
22. Gupta M, Maurer MJ, Wellik LE, et al. Expression of Myc, but not pSTAT3, is an adverse prognostic factor for diffuse large B-cell lymphoma treated with epratuzumab/R-CHOP. *Blood.* 2012;120(22):4400-4406.
23. Pfeifer M, Grau M, Lenze D, et al. PTEN loss defines a PI3K/AKT pathway-dependent germinal center subtype of diffuse large B-cell lymphoma. *Proc Natl Acad Sci USA.* 2013;110(30):12420-12425.
24. Rui L, Emre NC, Kruhlak MJ, et al. Cooperative epigenetic modulation by cancer amplicon genes. *Cancer Cell.* 2010;18(6):590-605.
25. Yang Y, Shaffer AL III, Emre NC, et al. Exploiting synthetic lethality for the therapy of ABC diffuse large B cell lymphoma. *Cancer Cell.* 2012;21(6):723-737.
26. Marzec M, Halasa K, Liu X, et al. Malignant transformation of CD4+ T lymphocytes mediated by oncogenic kinase NPM/ALK recapitulates IL-2-induced cell signaling and gene expression reprogramming. *J Immunol.* 2013;191(12):6200-6207.
27. Shaffer AL, Wright G, Yang L, et al. A library of gene expression signatures to illuminate normal and pathological lymphoid biology. *Immunol Rev.* 2006;210:67-85.
28. Subramanian A, Tamayo P, Mootha VK, et al. Gene set enrichment analysis: a knowledge-based approach for interpreting genome-wide expression profiles. *Proc Natl Acad Sci USA.* 2005;102(43):15545-15550.
29. Liberzon A, Subramanian A, Pinchback R, Thorvaldsdóttir H, Tamayo P, Mesirov JP. Molecular signatures database (MSigDB) 3.0. *Bioinformatics.* 2011;27(12):1739-1740.
30. Delmore JE, Issa GC, Lemieux ME, et al. BET bromodomain inhibition as a therapeutic strategy to target c-Myc. *Cell.* 2011;146(6):904-917.
31. Mertz JA, Conery AR, Bryant BM, et al. Targeting MYC dependence in cancer by inhibiting BET bromodomains. *Proc Natl Acad Sci USA.* 2011;108(40):16669-16674.
32. Dib A, Gabrea A, Glebov O, Bergsagel PL, Kuehl WM. Characterization of MYC translocations in multiple myeloma cell lines. *J Natl Cancer Inst Monogr.* 2008;(39)25-31.
33. Yin X, Giap C, Lazo JS, Prochownik EV. Low molecular weight inhibitors of Myc-Max interaction and function. *Oncogene.* 2003;22(40):6151-6159.
34. Davis RE, Brown KD, Siebenlist U, Staudt LM. Constitutive nuclear factor kappaB activity is required for survival of activated B cell-like diffuse large B cell lymphoma cells. *J Exp Med.* 2001;194(12):1861-1874.
35. Saito M, Gao J, Basso K, et al. A signaling pathway mediating downregulation of BCL6 in germinal center B cells is blocked by BCL6 gene alterations in B cell lymphoma. *Cancer Cell.* 2007;12(3):280-292.
36. Horie R, Watanabe M, Ishida T, et al. The NPM-ALK oncoprotein abrogates CD30 signaling and constitutive NF-kappaB activation in anaplastic large cell lymphoma. *Cancer Cell.* 2004;5(4):353-364.
37. Meyer N, Penn LZ. Reflecting on 25 years with MYC. *Nat Rev Cancer.* 2008;8(12):976-990.
38. Raetz EA, Perkins SL, Carlson MA, Schooler KP, Carroll WL, Virshup DM. The nucleophosmin-anaplastic lymphoma kinase fusion protein induces c-Myc expression in pediatric anaplastic large cell lymphomas. *Am J Pathol.* 2002;161(3):875-883.
39. Monaco S, Tsao L, Murty VV, et al. Pediatric ALK+ anaplastic large cell lymphoma with t(3;8)(q26.2;q24) translocation and c-myc rearrangement terminating in a leukemic phase. *Am J Hematol.* 2007;82(1):59-64.
40. Liang X, Branchford B, Greffe B, et al. Dual ALK and MYC rearrangements leading to an aggressive variant of anaplastic large cell lymphoma. *J Pediatr Hematol Oncol.* 2013;35(5):e209-e213.
41. Inghirami G, Macri L, Cesarman E, Chadburn A, Zhong J, Knowles DM. Molecular characterization of CD30+ anaplastic large-cell lymphoma: high frequency of c-myc proto-oncogene activation. *Blood.* 1994;83(12):3581-3590.
42. Boi M, Rinaldi A, Kwee I, et al. PRDM1/BLIMP1 is commonly inactivated in anaplastic large T-cell lymphoma. *Blood.* 2013;122(15):2683-2693.
43. Sibon D, Fournier M, Brière J, et al. Long-term outcome of adults with systemic anaplastic large-cell lymphoma treated within the Groupe d'Etude des Lymphomes de l'Adulte trials. *J Clin Oncol.* 2012;30(32):3939-3946.

Essential role of IRF4 and MYC signaling for survival of anaplastic large cell lymphoma

Supplemental Material and Methods

In vivo xenograft mouse studies

For *in vivo* testing of the K299 and JB6 xenograft mouse models, 6-8 week old female NOD.Cg-Prkdc scid Il2rgtm1Wjl/SzJ (NSG, Jackson Laboratory) mice were used. The mice were held in individually ventilated cages (IVC) under sterile and standardized environmental conditions (25 ± 2°C room temperature, 50 ± 10% relative humidity, 12h light–dark-rhythm). The mice received autoclaved food and bedding (ssniff, Soest) and acidified (pH 4.0) drinking water ad libitum. All animal experiments were conducted in accordance with the UKCCCR guidelines for the welfare of animals and the German animal protection law.

K299 and JB6 cells (1x10*^{7}/mouse) were mixed with matrigel and six (K299) and three (JB6) mice respectively per group were subcutaneously (s.c.) transplanted into the left flank region on day zero. To induce either *IRF4* shRNA #1 or the non-toxic shRNA directed against *MSMO1*, mice received drinking water supplemented with 1 mg/ml Doxycycline (Genaxxon) and 5% sucrose at day five of palpable tumors of approximately 30 mm^{3}. Tumor size was measured three times weekly in two dimensions using caliper and tumor volume (V) was calculated according to the following formula 1/2 x (length x width^{2}). The experiment was terminated on day 14. Tumor biopsies for Western blotting were obtained after termination of the experiment.

Gene expression profiling

Gene expression profiling was performed 24, 48, 72 and 96 hours following *IRF4* shRNA #1 induction. Total RNA was isolated using the NucleoSpin RNA II Kit (Macherey & Nagel) according to the manufacturer's protocol. RNA was amplified and labeled with the TotalPrep RNA Amplification Kit (Illumina). Samples were subsequently hybridized on HumanHT-12 v4 Expression BeadChips (Illumina) following the manufacturer's protocol as previously described.[1, 2] The gene expression data has been deposited in the GEO database (http://www.ncbi.nlm.nih.gov/geo/; accession number GSE59747).

Gene expression changes in cells in which *IRF4* shRNA #1 was induced with doxycycline were compared to uninduced cells. All microarrays were preprocessed and normalized together. The intensity distributions were equalized by quantile normalization for all measured beads. The background mode was fitted and removed and a spot filter was applied to exclude too dim beads (< mean background intensity). Intensities were log2-transformed and aggregated by measured sequence to form beadsets. Beadsets with more than 50% of their beads excluded by the spot filter were also excluded. Further analysis was performed on gene level using manufacturer’s annotations. For genes having multiple beadsets the one with the highest signal brightness (in average over all arrays) was selected.

Differentially expressed genes were identified in the following manner. A one-tailed paired t-test was used to calculate p-values for every gene based on the 12 microarray pairs. Additionally we used the Benjamini & Hochberg method to calculate a false discovery rate (FDR) for every significance threshold. We identified 115 genes that were significantly downregulated ($p<0.0025$; FDR=0.08) and 211 genes that were upregulated ($p<0.0025$; FDR=0.09) across all time points and all three cell lines following IRF4 knockdown (Supplemental Table 2).

To obtain a better understanding of the gene expression changes, we performed an unbiased gene set enrichment analysis (GSEA) as described for the IRF4 gene expression dataset using a previously described signature database.[3, 4] This analysis suggested significant downregulation of MYC target gene signatures. To validate this finding, we selected additional biologically linked MYC target gene signatures from the Molecular Signatures Database.[5]

Western blotting

Western blotting was performed as described.[6] The protein amount was quantified using the BCA assay (Thermo Scientific). Antibodies used in this study were obtained from Cell Signaling (IRF4), Abcam (MYC) and Sigma-Aldrich (Tubulin).

Chromatin Immunoprecipitation (ChIP)

ChIP was performed in the ALK+ ALCL cell line DEL and the ALK- ALCL cell line FE-PD. 20-40*10^6 cells were cross-linked with 1% formaldehyde on a shaking platform for 10 minutes at room temperature and the cross-linking reaction was stopped by incubation with 0.125 M glycine for 5 minutes at room temperature. Cells were then washed two times in PBS, resuspended in ChIP lysis buffer (50 mM HEPES, 150 mM NaCl, 1% Triton-X 100, 0.1% Na-deoxycholate, 1 mM EDTA) supplemented with SDS (0.25% final) and protease inhibitor cocktail (Roche), incubated on ice for 1 hour, and sonicated for 13 cycles (each for 1 minute at 80% duty cycle and 80% power output) with an MS72 tip-fitted Bandelin Sonoplus HD2070 sonicator. Sonicated lysates were cleared by centrifugation for 5 minutes at 13.000 rounds per minute (rpm). Soluble chromatin lysate - derived from 5*10^6 cells - was diluted three-fold with ChIP lysis buffer with protease inhibitor cocktail, and was incubated with 50 µl of an equal volume mix of Protein G and Protein A magnetic beads (Dynal, Life

Technologies) pre-bound with 5 µg anti-IRF4 antibody (Santa Cruz; sc-6059) or normal goat IgG (Santa Cruz; sc-2028) for 45 minutes at room temperature. Bead-bound immune complexes were then washed 6 times each for 1 minute at room temperature with shaking using 0.8 ml of the following: ChIP lysis buffer (2 times), ChIP lysis buffer with 500 mM NaCl (2 times), and TE (2 times). These washed, bead-bound immune complexes, and corresponding sonicated lysate (to be used as non-enriched "input control") were then boiled for 10 minutes in TE, treated with RNase A (Sigma-Aldrich; 0.1 µg/µl final) for 45 minutes at 39°C, treated with Proteinase K (Sigma-Aldrich; 200 ng/µl final) for 30 minutes at 55°C, boiled again for 10 minutes, and the DNA residing in the supernatant was purified using silica-based spin columns (Macherey Nagel).

Purified enriched DNA and input control DNA were then diluted 25- to 100-fold, and subjected to real-time PCR (qPCR) amplification in triplicates with previously described *MYC* and control specific primer pairs[7] (sequences given in Supplemental Table 1) on a PikoReal instrument (Thermo Scientific). The control locus is a region on chromosome 7, used as a negative control for IRF4 binding, due to lack of observable IRF4 binding in previous studies.[7, 8] qPCR reactions without template DNA were set up for each primer pair in order to rule out DNA contaminations or unspecific amplifications. The resulting qPCR data from each ChIP experiment were then analyzed with the ΔΔCt method, normalized to corresponding data of input DNA samples, and plotted.

References

1. Nogai H, Wenzel SS, Hailfinger S, et al. IkappaB-zeta controls the constitutive NF-kappaB target gene network and survival of ABC DLBCL. *Blood.* Sep 26 2013;122(13):2242-2250.

2. Pfeifer M, Grau M, Lenze D, et al. PTEN loss defines a PI3K/AKT pathway-dependent germinal center subtype of diffuse large B-cell lymphoma. *Proc Natl Acad Sci U S A.* Jul 9 2013.

3. Subramanian A, Tamayo P, Mootha VK, et al. From the Cover: Gene set enrichment analysis: A knowledge-based approach for interpreting genome-wide expression profiles. *Proc Natl Acad Sci U S A.* Oct 25 2005;102(43):15545-15550.

4. Shaffer AL, Wright G, Yang L, et al. A library of gene expression signatures to illuminate normal and pathological lymphoid biology. *Immunol Rev.* Apr 2006;210:67-85.

5. Liberzon A, Subramanian A, Pinchback R, Thorvaldsdottir H, Tamayo P, Mesirov JP. Molecular signatures database (MSigDB) 3.0. *Bioinformatics.* Jun 15 2011;27(12):1739-1740.

6. Wenzel SS, Grau M, Mavis C, et al. MCL1 is deregulated in subgroups of diffuse large B-cell lymphoma. *Leukemia.* Jun 2013;27(6):1381-1390.

7. Rui L, Emre NC, Kruhlak MJ, et al. Cooperative epigenetic modulation by cancer amplicon genes. *Cancer Cell.* Dec 14 2010;18(6):590-605.

8. Yang Y, Shaffer AL, 3rd, Emre NC, et al. Exploiting synthetic lethality for the therapy of ABC diffuse large B cell lymphoma. *Cancer Cell.* Jun 12 2012;21(6):723-737.

Supplemental Figures

Supplemental Figure 1: ALCLs are addicted to IRF4.

A. *IRF4* shRNA #1 and #2 downregulate IRF4 protein in SU-DHL-1 cells measured by Western blotting.

B. A previously described non-toxic shRNA against *MSMO1* does not induce toxicity in MM, ALCL, SS, or T-ALL cell lines.

Supplemental Figure 2: IRF4 downregulation suppresses the gene expression network of MYC in ALCL.

A. IRF4 knockdown significantly downregulates the previously identified MYC target gene signature “Myc_overexpression_1.5x_up”. Changes of gene expression were

profiled at the indicated timepoints following induction of *IRF4* shRNA #1. Gene expression changes are depicted according to the color scale shown.

B. Gene set enrichment analysis of the previously described MYC gene expression signature “Schuhmacher_MYC_Targets_up”. This MYC signature is significantly enriched with downregulated genes following IRF4 knockdown.

Supplemental Figure 3: MYC might represent a therapeutic target for ALCL treatment.

ALCL cell lines are sensitive to MYC inhibition using the small molecule inhibitor 10058-F4 that inhibits MYC-MAX heterodimerization. Representative results of three replicates are shown.

Weilemann et al. Supplemental Figure 1

A

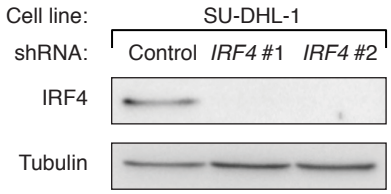

B

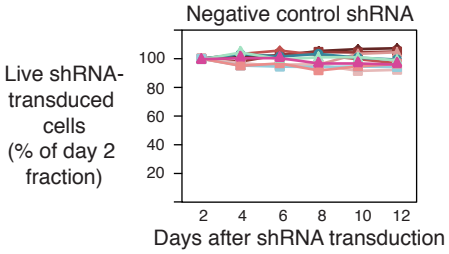

Cell line	Lymphoma/ leukemia subtype	*ALK* translocation status	IRF4 status
H929	MM	-	++
K299	ALCL	+	+++
JB6	ALCL	+	+++
DEL	ALCL	+	++
SU-DHL-1	ALCL	+	+
Mac-2A	ALCL	-	++
FE-PD	ALCL	-	+++
HuT 78	SS	-	+
Jurkat	T-ALL	-	-
KE-37	T-ALL	-	-

Weilemann et al. Supplemental Figure 2

A

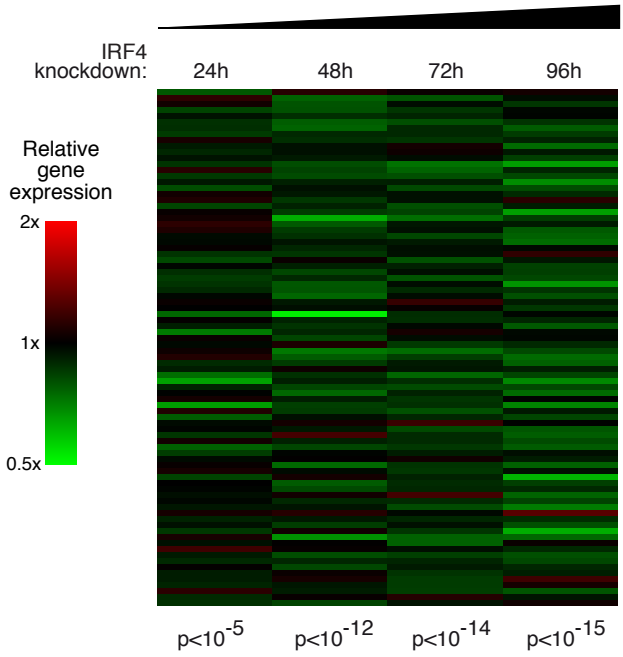

B

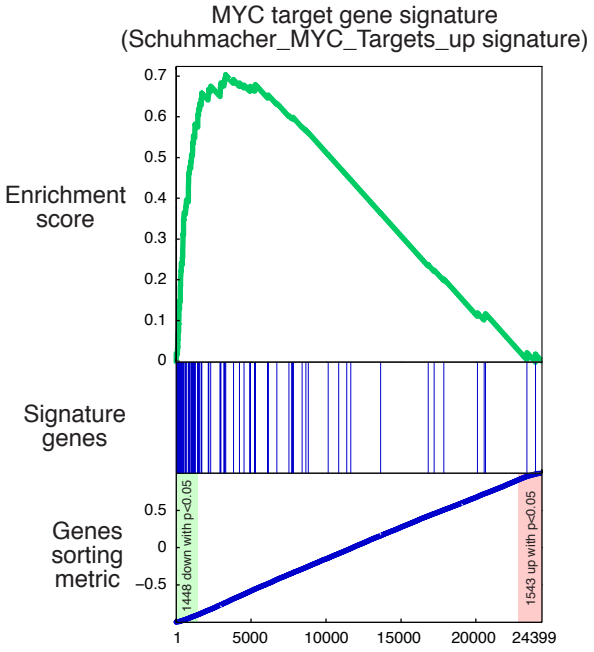

Weilemann et al. Supplemental Figure 3

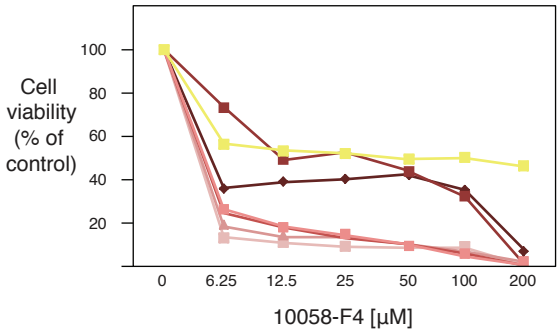

Cell line	Lymphoma subtype	MYC status
K299	ALCL	+
JB6	ALCL	+
DEL	ALCL	+
SU-DHL-1	ALCL	++
Mac-2A	ALCL	+
FE-PD	ALCL	+
U266	MM	-

Supplemental Table 1: Primers used for real-time PCR following IRF4 chromatin immunoprecipitation.

Target	Primer sequence
Myc Promoter - 0.4 kb	Forward-5': GGAGGGCAGCTGTTCCGCCTGCGATGA
	Reverse-5': AAACCGCATCCTTGTCCTGTGAGTATAAA
Myc Promoter + 0.3 kb	Forward-5': GCCTCTGGCCCAGCCCTCCCGCTGAT
	Reverse-5': GCAAAGTGCCCGCCCGCTGCTATGG
Negative control	Forward-5': AATATGTACATCAGGCAATCGGCTCTTC
	Reverse-5': CAACTGGAATCAGATCCACTTCATGGAAA

Supplemental Table 2: Downregulated and upregulated genes following IRF4 knockdown.

Signature name	Gene symbol	Gene ID	Gene description
IRF4shRNA_down_alpha=0.0025	ABHD6	57406	abhydrolase domain containing 6
IRF4shRNA_down_alpha=0.0025	ACSS1	84532	acyl-CoA synthetase short-chain family member 1
IRF4shRNA_down_alpha=0.0025	ALB	213	albumin
IRF4shRNA_down_alpha=0.0025	ARIH2	10425	ariadne homolog 2 (Drosophila)
IRF4shRNA_down_alpha=0.0025	BAG2	9532	BCL2-associated athanogene 2
IRF4shRNA_down_alpha=0.0025	BBS2	583	Bardet-Biedl syndrome 2
IRF4shRNA_down_alpha=0.0025	C16orf59	80178	chromosome 16 open reading frame 59
IRF4shRNA_down_alpha=0.0025	CAPN14	440854	calpain 14
IRF4shRNA_down_alpha=0.0025	CCDC86	79080	coiled-coil domain containing 86
IRF4shRNA_down_alpha=0.0025	CCR7	1236	chemokine (C-C motif) receptor 7
IRF4shRNA_down_alpha=0.0025	CD59	966	CD59 molecule, complement regulatory protein
IRF4shRNA_down_alpha=0.0025	CELF1	10658	CUGBP, Elav-like family member 1
IRF4shRNA_down_alpha=0.0025	CHST4	10164	carbohydrate (N-acetylglucosamine 6-O) sulfotransferase 4
IRF4shRNA_down_alpha=0.0025	CIRH1A	84916	cirrhosis, autosomal recessive 1A (cirhin)
IRF4shRNA_down_alpha=0.0025	CRABP2	1382	cellular retinoic acid binding protein 2
IRF4shRNA_down_alpha=0.0025	CTTN	2017	cortactin
IRF4shRNA_down_alpha=0.0025	DACH1	1602	dachshund homolog 1 (Drosophila)
IRF4shRNA_down_alpha=0.0025	DAG1	1605	dystroglycan 1 (dystrophin-associated glycoprotein 1)
IRF4shRNA_down_alpha=0.0025	DBNDD1	79007	dysbindin (dystrobrevin binding protein 1) domain containing 1
IRF4shRNA_down_alpha=0.0025	DDN	23109	dendrin
IRF4shRNA_down_alpha=0.0025	DHRS11	79154	dehydrogenase/reductase (SDR family) member 11
IRF4shRNA_down_alpha=0.0025	DMRT1	1761	doublesex and mab-3 related transcription factor 1
IRF4shRNA_down_alpha=0.0025	E2F6	1876	E2F transcription factor 6
IRF4shRNA_down_alpha=0.0025	EEA1	8411	early endosome antigen 1
IRF4shRNA_down_alpha=0.0025	EIF2C2	27161	eukaryotic translation initiation factor 2C, 2
IRF4shRNA_down_alpha=0.0025	EIF2S2	8894	eukaryotic translation initiation factor 2, subunit 2 beta, 38kDa
IRF4shRNA_down_alpha=0.0025	FAM161B	145483	family with sequence similarity 161, member B
IRF4shRNA_down_alpha=0.0025	FAM86C2P	645332	family with sequence similarity 86, member A pseudogene
IRF4shRNA_down_alpha=0.0025	FAM86JP	100125556	family with sequence similarity 86, member A pseudogene
IRF4shRNA_down_alpha=0.0025	FBXO44	93611	F-box protein 44
IRF4shRNA_down_alpha=0.0025	FJX1	24147	four jointed box 1 (Drosophila)
IRF4shRNA_down_alpha=0.0025	GATC	283459	glutamyl-tRNA(Gln) amidotransferase, subunit C homolog (bacterial)
IRF4shRNA_down_alpha=0.0025	GNL3	26354	guanine nucleotide binding protein-like 3 (nucleolar)
IRF4shRNA_down_alpha=0.0025	GNPDA1	10007	glucosamine-6-phosphate deaminase 1
IRF4shRNA_down_alpha=0.0025	HEATR1	55127	HEAT repeat containing 1

IRF4shRNA_down_alpha=0.0025	HES7	84667	hairy and enhancer of split 7 (Drosophila)
IRF4shRNA_down_alpha=0.0025	HK2P1	642546	hexokinase 2 pseudogene 1
IRF4shRNA_down_alpha=0.0025	HSPH1	10808	heat shock 105kDa/110kDa protein 1
IRF4shRNA_down_alpha=0.0025	IL2RA	3559	interleukin 2 receptor, alpha
IRF4shRNA_down_alpha=0.0025	ING5	84289	inhibitor of growth family, member 5
IRF4shRNA_down_alpha=0.0025	IRF4	3662	interferon regulatory factor 4
IRF4shRNA_down_alpha=0.0025	ITK	3702	IL2-inducible T-cell kinase
IRF4shRNA_down_alpha=0.0025	KIAA0020	9933	KIAA0020
IRF4shRNA_down_alpha=0.0025	KIAA0895	23366	KIAA0895
IRF4shRNA_down_alpha=0.0025	LGALSL	29094	lectin, galactoside-binding-like
IRF4shRNA_down_alpha=0.0025	LIG3	3980	ligase III, DNA, ATP-dependent
IRF4shRNA_down_alpha=0.0025	LOC100128881	100128881	uncharacterized LOC100128881
IRF4shRNA_down_alpha=0.0025	LOC442727	442727	prothymosin, alpha pseudogene
IRF4shRNA_down_alpha=0.0025	LOC728026	728026	prothymosin alpha-like
IRF4shRNA_down_alpha=0.0025	LYRM5	144363	LYR motif containing 5
IRF4shRNA_down_alpha=0.0025	MAK	4117	male germ cell-associated kinase
IRF4shRNA_down_alpha=0.0025	MFSD6L	162387	major facilitator superfamily domain containing 6-like
IRF4shRNA_down_alpha=0.0025	MINA	84864	MYC induced nuclear antigen
IRF4shRNA_down_alpha=0.0025	MMP20	9313	matrix metallopeptidase 20
IRF4shRNA_down_alpha=0.0025	MN1	4330	meningioma (disrupted in balanced translocation) 1
IRF4shRNA_down_alpha=0.0025	NAA10	8260	N(alpha)-acetyltransferase 10, NatA catalytic subunit
IRF4shRNA_down_alpha=0.0025	NAA15	80155	N(alpha)-acetyltransferase 15, NatA auxiliary subunit
IRF4shRNA_down_alpha=0.0025	NAA25	80018	N(alpha)-acetyltransferase 25, NatB auxiliary subunit
IRF4shRNA_down_alpha=0.0025	NARG2	79664	NMDA receptor regulated 2
IRF4shRNA_down_alpha=0.0025	NME2	4831	NME/NM23 nucleoside diphosphate kinase 2
IRF4shRNA_down_alpha=0.0025	NSMAF	8439	neutral sphingomyelinase (N-SMase) activation associated factor
IRF4shRNA_down_alpha=0.0025	OAF	220323	OAF homolog (Drosophila)
IRF4shRNA_down_alpha=0.0025	OTUD6B	51633	OTU domain containing 6B
IRF4shRNA_down_alpha=0.0025	PANX2	56666	pannexin 2
IRF4shRNA_down_alpha=0.0025	PIGA	5277	phosphatidylinositol glycan anchor biosynthesis, class A
IRF4shRNA_down_alpha=0.0025	PIK3R6	146850	phosphoinositide-3-kinase, regulatory subunit 6
IRF4shRNA_down_alpha=0.0025	PKP4	8502	plakophilin 4
IRF4shRNA_down_alpha=0.0025	PLD6	201164	phospholipase D family, member 6
IRF4shRNA_down_alpha=0.0025	POLD2P1	391811	polymerase (DNA directed), delta 2, accessory subunit pseudogene 1
IRF4shRNA_down_alpha=0.0025	POLG2	11232	polymerase (DNA directed), gamma 2, accessory subunit
IRF4shRNA_down_alpha=0.0025	PP7080	25845	uncharacterized LOC25845
IRF4shRNA_down_alpha=0.0025	PPAN	56342	peter pan homolog (Drosophila)
IRF4shRNA_down_alpha=0.0025	PTMA	5757	prothymosin, alpha

IRF4shRNA_down_alpha=0.0025	PTMAP8	728873	prothymosin, alpha pseudogene 8
IRF4shRNA_down_alpha=0.0025	PUS1	80324	pseudouridylate synthase 1
IRF4shRNA_down_alpha=0.0025	RIOK1	83732	RIO kinase 1 (yeast)
IRF4shRNA_down_alpha=0.0025	RPS6KA5	9252	ribosomal protein S6 kinase, 90kDa, polypeptide 5
IRF4shRNA_down_alpha=0.0025	S100A9	6280	S100 calcium binding protein A9
IRF4shRNA_down_alpha=0.0025	SFXN2	118980	sideroflexin 2
IRF4shRNA_down_alpha=0.0025	SLC16A7	9194	solute carrier family 16, member 7 (monocarboxylic acid transporter 2)
IRF4shRNA_down_alpha=0.0025	SLC19A3	80704	solute carrier family 19, member 3
IRF4shRNA_down_alpha=0.0025	SLC25A39	51629	solute carrier family 25, member 39
IRF4shRNA_down_alpha=0.0025	SLC37A3	84255	solute carrier family 37 (glycerol-3-phosphate transporter), member 3
IRF4shRNA_down_alpha=0.0025	SLC45A3	85414	solute carrier family 45, member 3
IRF4shRNA_down_alpha=0.0025	SLC4A7	9497	solute carrier family 4, sodium bicarbonate cotransporter, member 7
IRF4shRNA_down_alpha=0.0025	SNAPC5	10302	small nuclear RNA activating complex, polypeptide 5, 19kDa
IRF4shRNA_down_alpha=0.0025	SNORD31	9298	small nucleolar RNA, C/D box 31
IRF4shRNA_down_alpha=0.0025	SNORD6	692075	small nucleolar RNA, C/D box 6
IRF4shRNA_down_alpha=0.0025	SNX5	27131	sorting nexin 5
IRF4shRNA_down_alpha=0.0025	SOX2-OT	347689	SOX2 overlapping transcript (non-protein coding)
IRF4shRNA_down_alpha=0.0025	SPIN1	10927	spindlin 1
IRF4shRNA_down_alpha=0.0025	STK39	27347	serine threonine kinase 39
IRF4shRNA_down_alpha=0.0025	STRBP	55342	spermatid perinuclear RNA binding protein
IRF4shRNA_down_alpha=0.0025	SURF6	6838	surfeit 6
IRF4shRNA_down_alpha=0.0025	SYN1	6853	synapsin I
IRF4shRNA_down_alpha=0.0025	TEAD4	7004	TEA domain family member 4
IRF4shRNA_down_alpha=0.0025	TEX19	400629	testis expressed 19
IRF4shRNA_down_alpha=0.0025	TMEM241	85019	transmembrane protein 241
IRF4shRNA_down_alpha=0.0025	TMEM48	55706	transmembrane protein 48
IRF4shRNA_down_alpha=0.0025	TMTC3	160418	transmembrane and tetratricopeptide repeat containing 3
IRF4shRNA_down_alpha=0.0025	TOMM40	10452	translocase of outer mitochondrial membrane 40 homolog (yeast)
IRF4shRNA_down_alpha=0.0025	TP63	8626	tumor protein p63
IRF4shRNA_down_alpha=0.0025	TRIM61	391712	tripartite motif containing 61
IRF4shRNA_down_alpha=0.0025	TRMT6	51605	tRNA methyltransferase 6 homolog (S. cerevisiae)
IRF4shRNA_down_alpha=0.0025	TSKU	25987	tsukushi small leucine rich proteoglycan homolog (Xenopus laevis)
IRF4shRNA_down_alpha=0.0025	TYRO3	7301	TYRO3 protein tyrosine kinase
IRF4shRNA_down_alpha=0.0025	TYSND1	219743	trypsin domain containing 1
IRF4shRNA_down_alpha=0.0025	UTP15	84135	UTP15, U3 small nucleolar ribonucleoprotein, homolog (S. cerevisiae)
IRF4shRNA_down_alpha=0.0025	WDR77	79084	WD repeat domain 77
IRF4shRNA_down_alpha=0.0025	WSB2	55884	WD repeat and SOCS box containing 2
IRF4shRNA_down_alpha=0.0025	YAF2	10138	YY1 associated factor 2

IRF4shRNA_down_alpha=0.0025	ZNF138	7697	zinc finger protein 138
IRF4shRNA_down_alpha=0.0025	ZNF239	8187	zinc finger protein 239
IRF4shRNA_down_alpha=0.0025	ZNF324B	388569	zinc finger protein 324B
IRF4shRNA_down_alpha=0.0025	ZNF74	7625	zinc finger protein 74
IRF4shRNA_up_alpha=0.0025	ACAP1	9744	ArfGAP with coiled-coil, ankyrin repeat and PH domains 1
IRF4shRNA_up_alpha=0.0025	ADC	113451	arginine decarboxylase
IRF4shRNA_up_alpha=0.0025	AGT	183	angiotensinogen (serpin peptidase inhibitor, clade A, member 8)
IRF4shRNA_up_alpha=0.0025	AGXT2L2	85007	alanine-glyoxylate aminotransferase 2-like 2
IRF4shRNA_up_alpha=0.0025	AIF1L	83543	allograft inflammatory factor 1-like
IRF4shRNA_up_alpha=0.0025	AIM1	202	absent in melanoma 1
IRF4shRNA_up_alpha=0.0025	ANKDD1A	348094	ankyrin repeat and death domain containing 1A
IRF4shRNA_up_alpha=0.0025	ANKRD50	57182	ankyrin repeat domain 50
IRF4shRNA_up_alpha=0.0025	ANPEP	290	alanyl (membrane) aminopeptidase
IRF4shRNA_up_alpha=0.0025	ANXA1	301	annexin A1
IRF4shRNA_up_alpha=0.0025	ANXA2R	389289	annexin A2 receptor
IRF4shRNA_up_alpha=0.0025	APOL3	80833	apolipoprotein L, 3
IRF4shRNA_up_alpha=0.0025	ARHGAP9	64333	Rho GTPase activating protein 9
IRF4shRNA_up_alpha=0.0025	ARHGEF3	50650	Rho guanine nucleotide exchange factor (GEF) 3
IRF4shRNA_up_alpha=0.0025	ARHGEF6	9459	Rac/Cdc42 guanine nucleotide exchange factor (GEF) 6
IRF4shRNA_up_alpha=0.0025	ASAH2C	653365	N-acylsphingosine amidohydrolase (non-lysosomal ceramidase) 2C
IRF4shRNA_up_alpha=0.0025	ATM	472	ataxia telangiectasia mutated
IRF4shRNA_up_alpha=0.0025	ATP2B4	493	ATPase, Ca++ transporting, plasma membrane 4
IRF4shRNA_up_alpha=0.0025	BATF	10538	basic leucine zipper transcription factor, ATF-like
IRF4shRNA_up_alpha=0.0025	BTN2A1	11120	butyrophilin, subfamily 2, member A1
IRF4shRNA_up_alpha=0.0025	C15orf48	84419	chromosome 15 open reading frame 48
IRF4shRNA_up_alpha=0.0025	C16orf74	404550	chromosome 16 open reading frame 74
IRF4shRNA_up_alpha=0.0025	C1orf54	79630	chromosome 1 open reading frame 54
IRF4shRNA_up_alpha=0.0025	C5orf62	85027	chromosome 5 open reading frame 62
IRF4shRNA_up_alpha=0.0025	CACNA2D3	55799	calcium channel, voltage-dependent, alpha 2/delta subunit 3
IRF4shRNA_up_alpha=0.0025	CCM2	83605	cerebral cavernous malformation 2
IRF4shRNA_up_alpha=0.0025	CD300C	10871	CD300c molecule
IRF4shRNA_up_alpha=0.0025	CD68	968	CD68 molecule
IRF4shRNA_up_alpha=0.0025	CD82	3732	CD82 molecule
IRF4shRNA_up_alpha=0.0025	CDKN1A	1026	cyclin-dependent kinase inhibitor 1A (p21, Cip1)
IRF4shRNA_up_alpha=0.0025	CDKN2D	1032	cyclin-dependent kinase inhibitor 2D (p19, inhibits CDK4)
IRF4shRNA_up_alpha=0.0025	CELF2	10659	CUGBP, Elav-like family member 2
IRF4shRNA_up_alpha=0.0025	CFLAR	8837	CASP8 and FADD-like apoptosis regulator

IRF4shRNA_up_alpha=0.0025	CHODL	140578	chondrolectin
IRF4shRNA_up_alpha=0.0025	CHRNB1	1140	cholinergic receptor, nicotinic, beta 1 (muscle)
IRF4shRNA_up_alpha=0.0025	CHSY1	22856	chondroitin sulfate synthase 1
IRF4shRNA_up_alpha=0.0025	CITED2	10370	Cbp/p300-interacting transactivator, with Glu/Asp-rich carboxy-terminal domain, 2
IRF4shRNA_up_alpha=0.0025	CMTM3	123920	CKLF-like MARVEL transmembrane domain containing 3
IRF4shRNA_up_alpha=0.0025	CMTM6	54918	CKLF-like MARVEL transmembrane domain containing 6
IRF4shRNA_up_alpha=0.0025	COL9A2	1298	collagen, type IX, alpha 2
IRF4shRNA_up_alpha=0.0025	CSMD2	114784	CUB and Sushi multiple domains 2
IRF4shRNA_up_alpha=0.0025	CST7	8530	cystatin F (leukocystatin)
IRF4shRNA_up_alpha=0.0025	CTSB	1508	cathepsin B
IRF4shRNA_up_alpha=0.0025	CTSH	1512	cathepsin H
IRF4shRNA_up_alpha=0.0025	CYTH4	27128	cytohesin 4
IRF4shRNA_up_alpha=0.0025	DCUN1D3	123879	DCN1, defective in cullin neddylation 1, domain containing 3 (S. cerevisiae)
IRF4shRNA_up_alpha=0.0025	DEXI	28955	Dexi homolog (mouse)
IRF4shRNA_up_alpha=0.0025	DLGAP4	22839	discs, large (Drosophila) homolog-associated protein 4
IRF4shRNA_up_alpha=0.0025	DVL3	1857	dishevelled, dsh homolog 3 (Drosophila)
IRF4shRNA_up_alpha=0.0025	ECM1	1893	extracellular matrix protein 1
IRF4shRNA_up_alpha=0.0025	EHBP1L1	254102	EH domain binding protein 1-like 1
IRF4shRNA_up_alpha=0.0025	ENPP1	5167	ectonucleotide pyrophosphatase/phosphodiesterase 1
IRF4shRNA_up_alpha=0.0025	EVI2B	2124	ecotropic viral integration site 2B
IRF4shRNA_up_alpha=0.0025	FAM129A	116496	family with sequence similarity 129, member A
IRF4shRNA_up_alpha=0.0025	FAM179A	165186	family with sequence similarity 179, member A
IRF4shRNA_up_alpha=0.0025	FAM214B	80256	family with sequence similarity 214, member B
IRF4shRNA_up_alpha=0.0025	FAM46A	55603	family with sequence similarity 46, member A
IRF4shRNA_up_alpha=0.0025	FAM89B	23625	family with sequence similarity 89, member B
IRF4shRNA_up_alpha=0.0025	FAS	355	Fas (TNF receptor superfamily, member 6)
IRF4shRNA_up_alpha=0.0025	FES	2242	feline sarcoma oncogene
IRF4shRNA_up_alpha=0.0025	FGF9	2254	fibroblast growth factor 9 (glia-activating factor)
IRF4shRNA_up_alpha=0.0025	FTH1P2	2497	ferritin, heavy polypeptide 1 pseudogene 2
IRF4shRNA_up_alpha=0.0025	FTH1P20	729009	ferritin, heavy polypeptide 1 pseudogene 20
IRF4shRNA_up_alpha=0.0025	FTH1P3	2498	ferritin, heavy polypeptide 1 pseudogene 3
IRF4shRNA_up_alpha=0.0025	FTH1P8	2501	ferritin, heavy polypeptide 1 pseudogene 8
IRF4shRNA_up_alpha=0.0025	FURIN	5045	furin (paired basic amino acid cleaving enzyme)
IRF4shRNA_up_alpha=0.0025	GAB3	139716	GRB2-associated binding protein 3
IRF4shRNA_up_alpha=0.0025	GADD45A	1647	growth arrest and DNA-damage-inducible, alpha
IRF4shRNA_up_alpha=0.0025	GALM	130589	galactose mutarotase (aldose 1-epimerase)
IRF4shRNA_up_alpha=0.0025	GALNT10	55568	UDP-N-acetyl-alpha-D-galactosamine:polypeptide N-acetylgalactosaminyltransferase 10 (GalNAc-T10)
IRF4shRNA_up_alpha=0.0025	GBP1	2633	guanylate binding protein 1, interferon-inducible

IRF4shRNA_up_alpha=0.0025	GBP1P1	400759	guanylate binding protein 1, interferon-inducible pseudogene 1
IRF4shRNA_up_alpha=0.0025	GPSM3	63940	G-protein signaling modulator 3
IRF4shRNA_up_alpha=0.0025	GVINP1	387751	GTPase, very large interferon inducible pseudogene 1
IRF4shRNA_up_alpha=0.0025	GYG1	2992	glycogenin 1
IRF4shRNA_up_alpha=0.0025	GZMB	3002	granzyme B (granzyme 2, cytotoxic T-lymphocyte-associated serine esterase 1)
IRF4shRNA_up_alpha=0.0025	H2AFJ	55766	H2A histone family, member J
IRF4shRNA_up_alpha=0.0025	HCST	10870	hematopoietic cell signal transducer
IRF4shRNA_up_alpha=0.0025	HDAC4	9759	histone deacetylase 4
IRF4shRNA_up_alpha=0.0025	HIST1H1C	3006	histone cluster 1, H1c
IRF4shRNA_up_alpha=0.0025	HIST1H2AC	8334	histone cluster 1, H2ac
IRF4shRNA_up_alpha=0.0025	HIST1H2AG	8969	histone cluster 1, H2ag
IRF4shRNA_up_alpha=0.0025	HIST1H2BD	3017	histone cluster 1, H2bd
IRF4shRNA_up_alpha=0.0025	HIST1H2BK	85236	histone cluster 1, H2bk
IRF4shRNA_up_alpha=0.0025	HIST1H4H	8365	histone cluster 1, H4h
IRF4shRNA_up_alpha=0.0025	HIST2H2AA3	8337	histone cluster 2, H2aa3
IRF4shRNA_up_alpha=0.0025	HIST2H2AA4	723790	histone cluster 2, H2aa4
IRF4shRNA_up_alpha=0.0025	HIST2H2BE	8349	histone cluster 2, H2be
IRF4shRNA_up_alpha=0.0025	HIST2H4A	8370	histone cluster 2, H4a
IRF4shRNA_up_alpha=0.0025	HMOX2	3163	heme oxygenase (decycling) 2
IRF4shRNA_up_alpha=0.0025	ID2	3398	inhibitor of DNA binding 2, dominant negative helix-loop-helix protein
IRF4shRNA_up_alpha=0.0025	IFI44	10561	interferon-induced protein 44
IRF4shRNA_up_alpha=0.0025	IGFBP7	3490	insulin-like growth factor binding protein 7
IRF4shRNA_up_alpha=0.0025	IL1RN	3557	interleukin 1 receptor antagonist
IRF4shRNA_up_alpha=0.0025	IL26	55801	interleukin 26
IRF4shRNA_up_alpha=0.0025	IL4I1	259307	interleukin 4 induced 1
IRF4shRNA_up_alpha=0.0025	IL4R	3566	interleukin 4 receptor
IRF4shRNA_up_alpha=0.0025	IL7R	3575	interleukin 7 receptor
IRF4shRNA_up_alpha=0.0025	IQGAP1	8826	IQ motif containing GTPase activating protein 1
IRF4shRNA_up_alpha=0.0025	ITGAV	3685	integrin, alpha V
IRF4shRNA_up_alpha=0.0025	ITM2B	9445	integral membrane protein 2B
IRF4shRNA_up_alpha=0.0025	ITPR1	3708	inositol 1,4,5-trisphosphate receptor, type 1
IRF4shRNA_up_alpha=0.0025	ITPRIP	85450	inositol 1,4,5-trisphosphate receptor interacting protein
IRF4shRNA_up_alpha=0.0025	KIAA0226L	80183	KIAA0226-like
IRF4shRNA_up_alpha=0.0025	KIAA0247	9766	KIAA0247
IRF4shRNA_up_alpha=0.0025	KIAA1217	56243	KIAA1217
IRF4shRNA_up_alpha=0.0025	KIR2DL1	3802	killer cell immunoglobulin-like receptor, two domains, long cytoplasmic tail, 1
IRF4shRNA_up_alpha=0.0025	KIR2DL3	3804	killer cell immunoglobulin-like receptor, two domains, long cytoplasmic tail, 3
IRF4shRNA_up_alpha=0.0025	KIR2DL4	3805	killer cell immunoglobulin-like receptor, two domains, long cytoplasmic tail, 4

IRF4shRNA_up_alpha=0.0025	KIR2DL5A	57292	killer cell immunoglobulin-like receptor, two domains, long cytoplasmic tail, 5A
IRF4shRNA_up_alpha=0.0025	KIR2DS5	3810	killer cell immunoglobulin-like receptor, two domains, short cytoplasmic tail, 5
IRF4shRNA_up_alpha=0.0025	KIR3DL1	3811	killer cell immunoglobulin-like receptor, three domains, long cytoplasmic tail, 1
IRF4shRNA_up_alpha=0.0025	KIR3DL2	3812	killer cell immunoglobulin-like receptor, three domains, long cytoplasmic tail, 2
IRF4shRNA_up_alpha=0.0025	KIR3DL3	115653	killer cell immunoglobulin-like receptor, three domains, long cytoplasmic tail, 3
IRF4shRNA_up_alpha=0.0025	KLF13	51621	Kruppel-like factor 13
IRF4shRNA_up_alpha=0.0025	KYNU	8942	kynureninase
IRF4shRNA_up_alpha=0.0025	LAPTM5	7805	lysosomal protein transmembrane 5
IRF4shRNA_up_alpha=0.0025	LAT2	7462	linker for activation of T cells family, member 2
IRF4shRNA_up_alpha=0.0025	LGALS1	3956	lectin, galactoside-binding, soluble, 1
IRF4shRNA_up_alpha=0.0025	LGALS3	3958	lectin, galactoside-binding, soluble, 3
IRF4shRNA_up_alpha=0.0025	LINC00260	84719	long intergenic non-protein coding RNA 260
IRF4shRNA_up_alpha=0.0025	LINC00294	283267	long intergenic non-protein coding RNA 294
IRF4shRNA_up_alpha=0.0025	LINC00341	79686	long intergenic non-protein coding RNA 341
IRF4shRNA_up_alpha=0.0025	LOC286453	286453	chondroitin sulfate N-acetylgalactosaminyltransferase 2 pseudogene
IRF4shRNA_up_alpha=0.0025	LOC550643	550643	uncharacterized LOC550643
IRF4shRNA_up_alpha=0.0025	LRRC8C	84230	leucine rich repeat containing 8 family, member C
IRF4shRNA_up_alpha=0.0025	MAML2	84441	mastermind-like 2 (Drosophila)
IRF4shRNA_up_alpha=0.0025	MEF2D	4209	myocyte enhancer factor 2D
IRF4shRNA_up_alpha=0.0025	METRNL	284207	meteorin, glial cell differentiation regulator-like
IRF4shRNA_up_alpha=0.0025	MIAT	440823	myocardial infarction associated transcript (non-protein coding)
IRF4shRNA_up_alpha=0.0025	MOAP1	64112	modulator of apoptosis 1
IRF4shRNA_up_alpha=0.0025	MTMR11	10903	myotubularin related protein 11
IRF4shRNA_up_alpha=0.0025	MTMR7	9108	myotubularin related protein 7
IRF4shRNA_up_alpha=0.0025	MXD1	4084	MAX dimerization protein 1
IRF4shRNA_up_alpha=0.0025	MYO1F	4542	myosin IF
IRF4shRNA_up_alpha=0.0025	NCF4	4689	neutrophil cytosolic factor 4, 40kDa
IRF4shRNA_up_alpha=0.0025	NFKBIZ	64332	nuclear factor of kappa light polypeptide gene enhancer in B-cells inhibitor, zeta
IRF4shRNA_up_alpha=0.0025	NLRP7	199713	NLR family, pyrin domain containing 7
IRF4shRNA_up_alpha=0.0025	NMRK1	54981	nicotinamide riboside kinase 1
IRF4shRNA_up_alpha=0.0025	NUB1	51667	negative regulator of ubiquitin-like proteins 1
IRF4shRNA_up_alpha=0.0025	NUCB2	4925	nucleobindin 2
IRF4shRNA_up_alpha=0.0025	OAS3	4940	2'-5'-oligoadenylate synthetase 3, 100kDa
IRF4shRNA_up_alpha=0.0025	ORAI3	93129	ORAI calcium release-activated calcium modulator 3
IRF4shRNA_up_alpha=0.0025	OSTF1	26578	osteoclast stimulating factor 1
IRF4shRNA_up_alpha=0.0025	PBX4	80714	pre-B-cell leukemia homeobox 4
IRF4shRNA_up_alpha=0.0025	PBXIP1	57326	pre-B-cell leukemia homeobox interacting protein 1
IRF4shRNA_up_alpha=0.0025	PCMTD1	115294	protein-L-isoaspartate (D-aspartate) O-methyltransferase domain containing 1

IRF4shRNA_up_alpha=0.0025	PHLDA1	22822	pleckstrin homology-like domain, family A, member 1
IRF4shRNA_up_alpha=0.0025	PIK3CG	5294	phosphatidylinositol-4,5-bisphosphate 3-kinase, catalytic subunit gamma
IRF4shRNA_up_alpha=0.0025	PLXNC1	10154	plexin C1
IRF4shRNA_up_alpha=0.0025	POU3F2	5454	POU class 3 homeobox 2
IRF4shRNA_up_alpha=0.0025	PPP1R18	170954	protein phosphatase 1, regulatory subunit 18
IRF4shRNA_up_alpha=0.0025	PPP1R27	116729	protein phosphatase 1, regulatory subunit 27
IRF4shRNA_up_alpha=0.0025	PRDM8	56978	PR domain containing 8
IRF4shRNA_up_alpha=0.0025	PRF1	5551	perforin 1 (pore forming protein)
IRF4shRNA_up_alpha=0.0025	PTPN22	26191	protein tyrosine phosphatase, non-receptor type 22 (lymphoid)
IRF4shRNA_up_alpha=0.0025	PXN	5829	paxillin
IRF4shRNA_up_alpha=0.0025	RAB32	10981	RAB32, member RAS oncogene family
IRF4shRNA_up_alpha=0.0025	RAB8B	51762	RAB8B, member RAS oncogene family
IRF4shRNA_up_alpha=0.0025	RAC2	5880	ras-related C3 botulinum toxin substrate 2 (rho family, small GTP binding protein Rac2)
IRF4shRNA_up_alpha=0.0025	RASD1	51655	RAS, dexamethasone-induced 1
IRF4shRNA_up_alpha=0.0025	RASL11B	65997	RAS-like, family 11, member B
IRF4shRNA_up_alpha=0.0025	RCAN2	10231	regulator of calcineurin 2
IRF4shRNA_up_alpha=0.0025	RELA	5970	v-rel reticuloendotheliosis viral oncogene homolog A (avian)
IRF4shRNA_up_alpha=0.0025	RHOC	389	ras homolog family member C
IRF4shRNA_up_alpha=0.0025	RHOU	58480	ras homolog family member U
IRF4shRNA_up_alpha=0.0025	RNASEL	6041	ribonuclease L (2',5'-oligoisoadenylate synthetase-dependent)
IRF4shRNA_up_alpha=0.0025	RNF114	55905	ring finger protein 114
IRF4shRNA_up_alpha=0.0025	RRN3P1	730092	RNA polymerase I transcription factor homolog (S. cerevisiae) pseudogene 1
IRF4shRNA_up_alpha=0.0025	RTP4	64108	receptor (chemosensory) transporter protein 4
IRF4shRNA_up_alpha=0.0025	S100P	6286	S100 calcium binding protein P
IRF4shRNA_up_alpha=0.0025	SAMD9L	219285	sterile alpha motif domain containing 9-like
IRF4shRNA_up_alpha=0.0025	SATB1	6304	SATB homeobox 1
IRF4shRNA_up_alpha=0.0025	SBNO2	22904	strawberry notch homolog 2 (Drosophila)
IRF4shRNA_up_alpha=0.0025	SDC4	6385	syndecan 4
IRF4shRNA_up_alpha=0.0025	SERPINA1	5265	serpin peptidase inhibitor, clade A (alpha-1 antiproteinase, antitrypsin), member 1
IRF4shRNA_up_alpha=0.0025	SH2D2A	9047	SH2 domain containing 2A
IRF4shRNA_up_alpha=0.0025	SH3BGRL3	83442	SH3 domain binding glutamic acid-rich protein like 3
IRF4shRNA_up_alpha=0.0025	SH3BP2	6452	SH3-domain binding protein 2
IRF4shRNA_up_alpha=0.0025	SH3TC1	54436	SH3 domain and tetratricopeptide repeats 1
IRF4shRNA_up_alpha=0.0025	SLC9A9	285195	solute carrier family 9, subfamily A (NHE9, cation proton antiporter 9), member 9
IRF4shRNA_up_alpha=0.0025	SLFN12	55106	schlafen family member 12
IRF4shRNA_up_alpha=0.0025	SMOX	54498	spermine oxidase
IRF4shRNA_up_alpha=0.0025	SNTB1	6641	syntrophin, beta 1 (dystrophin-associated protein A1, 59kDa, basic component 1)
IRF4shRNA_up_alpha=0.0025	SPTLC2	9517	serine palmitoyltransferase, long chain base subunit 2

IRF4shRNA_up_alpha=0.0025	SRGN	5552	serglycin
IRF4shRNA_up_alpha=0.0025	STXBP2	6813	syntaxin binding protein 2
IRF4shRNA_up_alpha=0.0025	SURF4	6836	surfeit 4
IRF4shRNA_up_alpha=0.0025	TBC1D2B	23102	TBC1 domain family, member 2B
IRF4shRNA_up_alpha=0.0025	TCN2	6948	transcobalamin II
IRF4shRNA_up_alpha=0.0025	TLR6	10333	toll-like receptor 6
IRF4shRNA_up_alpha=0.0025	TMEM140	55281	transmembrane protein 140
IRF4shRNA_up_alpha=0.0025	TMEM173	340061	transmembrane protein 173
IRF4shRNA_up_alpha=0.0025	TMEM217	221468	transmembrane protein 217
IRF4shRNA_up_alpha=0.0025	TNFRSF1A	7132	tumor necrosis factor receptor superfamily, member 1A
IRF4shRNA_up_alpha=0.0025	TNFRSF1B	7133	tumor necrosis factor receptor superfamily, member 1B
IRF4shRNA_up_alpha=0.0025	TNFSF10	8743	tumor necrosis factor (ligand) superfamily, member 10
IRF4shRNA_up_alpha=0.0025	TNIK	23043	TRAF2 and NCK interacting kinase
IRF4shRNA_up_alpha=0.0025	TOX2	84969	TOX high mobility group box family member 2
IRF4shRNA_up_alpha=0.0025	TPST2	8459	tyrosylprotein sulfotransferase 2
IRF4shRNA_up_alpha=0.0025	TRANK1	9881	tetratricopeptide repeat and ankyrin repeat containing 1
IRF4shRNA_up_alpha=0.0025	TRIM9	114088	tripartite motif containing 9
IRF4shRNA_up_alpha=0.0025	TWIST1	7291	twist homolog 1 (Drosophila)
IRF4shRNA_up_alpha=0.0025	UCN2	90226	urocortin 2
IRF4shRNA_up_alpha=0.0025	VAV1	7409	vav 1 guanine nucleotide exchange factor
IRF4shRNA_up_alpha=0.0025	VIM	7431	vimentin
IRF4shRNA_up_alpha=0.0025	WASF2	10163	WAS protein family, member 2
IRF4shRNA_up_alpha=0.0025	WBP1L	54838	WW domain binding protein 1-like
IRF4shRNA_up_alpha=0.0025	YPEL5	51646	yippee-like 5 (Drosophila)
IRF4shRNA_up_alpha=0.0025	ZBTB16	7704	zinc finger and BTB domain containing 16
IRF4shRNA_up_alpha=0.0025	ZEB2	9839	zinc finger E-box binding homeobox 2

Supplemental Table 3: Signatures that are significantly enriched with top regulated genes after IRF4 knockdown.

Downregulated signatures:

Category	Signature name	Signature links	Defined members	Enrich-ment score	p [GSEA] (by permutation test)	FDR [GSEA]
Signaling pathway	Myc_overexpression_1.5x_up	http://lymphochip.nih.gov/cgi-bin/signaturedb/signatureDB_DisplayGenes.cgi?signatureID=167	88	0,7593	0,0010	0,0010
Signaling pathway	Myc_overexpression_2x_up	http://lymphochip.nih.gov/cgi-bin/signaturedb/signatureDB_DisplayGenes.cgi?signatureID=168	36	0,7321	0,0010	0,0010
Transcription factor target	HIF1alpha_1.5x_down	http://lymphochip.nih.gov/cgi-bin/signaturedb/signatureDB_DisplayGenes.cgi?signatureID=193	215	0,6504	0,0010	0,0010
Transcription factor target	Myc_RNAi_OCILy3	http://lymphochip.nih.gov/cgi-bin/signaturedb/signatureDB_DisplayGenes.cgi?signatureID=80	54	0,6451	0,0010	0,0010
Cellular process	Proliferation_Node1640	http://lymphochip.nih.gov/cgi-bin/signaturedb/signatureDB_DisplayGenes.cgi?signatureID=114	56	0,6024	0,0010	0,0010
Cellular process	Proliferation_Node1618	http://lymphochip.nih.gov/cgi-bin/signaturedb/signatureDB_DisplayGenes.cgi?signatureID=113	58	0,6020	0,0009	0,0009
Signaling pathway	Notch_T-ALL_up_Palomero	http://lymphochip.nih.gov/cgi-bin/signaturedb/signatureDB_DisplayGenes.cgi?signatureID=235	47	0,5991	0,0010	0,0010
Cancer differential	MCL_proliferation_survival	http://lymphochip.nih.gov/cgi-bin/signaturedb/signatureDB_DisplayGenes.cgi?signatureID=46	17	0,5908	0,0592	0,0296
Transcription factor target	Myc_ChIP_PET_Expr_Up	http://lymphochip.nih.gov/cgi-bin/signaturedb/signatureDB_DisplayGenes.cgi?signatureID=245	405	0,5738	0,0010	0,0010
Transcription factor target	HIF1alpha_2x_down	http://lymphochip.nih.gov/cgi-bin/signaturedb/signatureDB_DisplayGenes.cgi?signatureID=194	41	0,5664	0,0024	0,0012
Cellular process	Glutamine_starve_down	http://lymphochip.nih.gov/cgi-bin/signaturedb/signatureDB_DisplayGenes.cgi?signatureID=137	313	0,5638	0,0010	0,0009
Signaling pathway	Notch_T-ALL_up_Sharma	http://lymphochip.nih.gov/cgi-bin/signaturedb/signatureDB_DisplayGenes.cgi?signatureID=228	37	0,5462	0,0089	0,0022
Cellular differentiation	CD8_T_effectorDn_memoryDn_Naiv	http://lymphochip.nih.gov/cgi-bin/signaturedb/signatureDB_DisplayGenes.cgi?signatureID=155	14	0,5248	0,2204	0,1102
Cellular differentiation	Erythrocytic_Node1660	http://lymphochip.nih.gov/cgi-bin/signaturedb/signatureDB_DisplayGenes.cgi?signatureID=100	14	0,5230	0,1354	0,2472
Cancer differential	Myeloma_PR_subgroup_up	http://lymphochip.nih.gov/cgi-bin/signaturedb/signatureDB_DisplayGenes.cgi?signatureID=212	49	0,5137	0,0104	0,0441
Cellular process	Leucine_starve_down	http://lymphochip.nih.gov/cgi-bin/signaturedb/signatureDB_DisplayGenes.cgi?signatureID=139	178	0,5088	0,0010	0,0010

Upregulated signatures:

Category	Signature name	Signature links	Defined members	Enrich-ment score	p [GSEA] (by permutation test)	FDR [GSEA]
Cellular process	Quiescence_heme_cluster3	http://lymphochip.nih.gov/cgi-bin/signaturedb/signatureDB_DisplayGenes.cgi?signatureID=55	12	-0,7423	0,0133	0,0044
Cellular differentiation	Hematopoietic_Node1658	http://lymphochip.nih.gov/cgi-bin/signaturedb/signatureDB_DisplayGenes.cgi?signatureID=101	84	-0,6492	0,0010	0,0010
Signaling pathway	Notch_T-ALL_down_Sharma	http://lymphochip.nih.gov/cgi-bin/signaturedb/signatureDB_DisplayGenes.cgi?signatureID=229	18	-0,6184	0,0311	0,0236
Cellular process	Quiescence_heme_cluster1	http://lymphochip.nih.gov/cgi-bin/signaturedb/signatureDB_DisplayGenes.cgi?signatureID=53	151	-0,6157	0,0010	0,0010
Cancer differential	BreastCa_70gene_Good	http://lymphochip.nih.gov/cgi-bin/signaturedb/signatureDB_DisplayGenes.cgi?signatureID=190	13	-0,6072	0,0693	0,0208
Cellular differentiation	T_NK_Node1604	http://lymphochip.nih.gov/cgi-bin/signaturedb/signatureDB_DisplayGenes.cgi?signatureID=117	20	-0,5975	0,0261	0,0500
Cellular differentiation	NK_U133plus	http://lymphochip.nih.gov/cgi-bin/signaturedb/signatureDB_DisplayGenes.cgi?signatureID=33	33	-0,5915	0,0031	0,0190
Signaling pathway	IFN_PMBC_4x_Up	http://lymphochip.nih.gov/cgi-bin/signaturedb/signatureDB_DisplayGenes.cgi?signatureID=162	82	-0,5697	0,0010	0,0010
Signaling pathway	TGFbeta_down_epithelial_large	http://lymphochip.nih.gov/cgi-bin/signaturedb/signatureDB_DisplayGenes.cgi?signatureID=234	20	-0,5670	0,0643	0,0193
Cellular differentiation	Regulatory_T_cell_McHugh_Herman	http://lymphochip.nih.gov/cgi-bin/signaturedb/signatureDB_DisplayGenes.cgi?signatureID=128	19	-0,5664	0,0915	0,0292
Cellular differentiation	T_NK_Node5808	http://lymphochip.nih.gov/cgi-bin/signaturedb/signatureDB_DisplayGenes.cgi?signatureID=196	20	-0,5660	0,0491	0,0721
Cellular differentiation	CNSonly_Node1460	http://lymphochip.nih.gov/cgi-bin/signaturedb/signatureDB_DisplayGenes.cgi?signatureID=97	18	-0,5621	0,0790	0,0406
Cellular process	Quiescence_heme_all	http://lymphochip.nih.gov/cgi-bin/signaturedb/signatureDB_DisplayGenes.cgi?signatureID=52	272	-0,5545	0,0010	0,0010
Cellular differentiation	T_cell	http://lymphochip.nih.gov/cgi-bin/signaturedb/signatureDB_DisplayGenes.cgi?signatureID=35	15	-0,5515	0,1691	0,0154
Transcription factor target	KLF2_induced	http://lymphochip.nih.gov/cgi-bin/signaturedb/signatureDB_DisplayGenes.cgi?signatureID=81	106	-0,5442	0,0010	0,0010
Transcription factor target	NFkB_Up_BCR_paper	http://lymphochip.nih.gov/cgi-bin/signaturedb/signatureDB_DisplayGenes.cgi?signatureID=274	68	-0,5324	0,0010	0,0010
Cancer differential	Myeloma_LB_subgroup_down	http://lymphochip.nih.gov/cgi-bin/signaturedb/signatureDB_DisplayGenes.cgi?signatureID=215	45	-0,5310	0,0085	0,0155
Cellular differentiation	Splenic_Marginal_zone_Bcell_gt_nai	http://lymphochip.nih.gov/cgi-bin/signaturedb/signatureDB_DisplayGenes.cgi?signatureID=44	24	-0,5280	0,0775	0,0182
Signaling pathway	Tcell_cytokine_induced_PMBConly_	http://lymphochip.nih.gov/cgi-bin/signaturedb/signatureDB_DisplayGenes.cgi?signatureID=76	42	-0,5274	0,0108	0,0281
Cancer differential	STAT3_up_OCILy10	http://lymphochip.nih.gov/cgi-bin/signaturedb/signatureDB_DisplayGenes.cgi?signatureID=252	42	-0,5234	0,0106	0,0151
Transcription factor target	STAT3_up_OCILy10	http://lymphochip.nih.gov/cgi-bin/signaturedb/signatureDB_DisplayGenes.cgi?signatureID=252	42	-0,5234	0,0095	0,0032
Cancer differential	Myeloma_CD-2_subgroup_up	http://lymphochip.nih.gov/cgi-bin/signaturedb/signatureDB_DisplayGenes.cgi?signatureID=222	47	-0,5233	0,0040	0,0359
Cellular differentiation	Resting_blood_NK_cell_GNF	http://lymphochip.nih.gov/cgi-bin/signaturedb/signatureDB_DisplayGenes.cgi?signatureID=39	71	-0,5212	0,0017	0,0175
Signaling pathway	JAK_IL10_Ly10_Up	http://lymphochip.nih.gov/cgi-bin/signaturedb/signatureDB_DisplayGenes.cgi?signatureID=258	39	-0,5104	0,0230	0,0185
Cellular differentiation	CD8_T_effectorUp_memoryUp_Naiv	http://lymphochip.nih.gov/cgi-bin/signaturedb/signatureDB_DisplayGenes.cgi?signatureID=154	31	-0,5071	0,0452	0,0543

Cancer differential	PMBL_HL_high	http://lymphochip.nih.gov/cgi-bin/signaturedb/signatureDB_DisplayGenes.cgi?signatureID=5	68	-0,5022	0,0010	0,0231
Signaling pathway	Tcell_cytokine_induced_PMBC_Bcel	http://lymphochip.nih.gov/cgi-bin/signaturedb/signatureDB_DisplayGenes.cgi?signatureID=75	31	-0,5016	0,0531	0,0076
Signaling pathway	IFN_PMBC_2x_Up	http://lymphochip.nih.gov/cgi-bin/signaturedb/signatureDB_DisplayGenes.cgi?signatureID=161	139	-0,5015	0,0010	0,0031
Cellular differentiation	Thymic_progenitor_Tcell_gt_Thymic_	http://lymphochip.nih.gov/cgi-bin/signaturedb/signatureDB_DisplayGenes.cgi?signatureID=26	30	-0,5006	0,0487	0,0440
Cancer differential	Follicular_lymphoma_Immune_Resp	http://lymphochip.nih.gov/cgi-bin/signaturedb/signatureDB_DisplayGenes.cgi?signatureID=132	41	-0,5001	0,0385	0,0064

Supplemental Table 4: MYC signatures analyzed for enrichment with top regulated genes after IRF4 knockdown.

Downregulated signatures:				
Signature name	**Signature links**	**Defined members**	**Enrich-ment score**	**p [GSEA] (by permutation test)**
Myc_overexpression_1.5x_up	http://lymphochip.nih.gov/cgi-bin/signaturedb/signatureDB_DisplayGenes.cgi?signatureID=167	86	0,7593	0,0010
SCHUHMACHER_MYC_TARGETS_UP	http://www.broadinstitute.org/gsea/msigdb/cards/SCHUHMACHER_MYC_TARGETS_UP	80	0,7030	0,0010
SCHLOSSER_MYC_AND_SERUM_RESPONSE_SYNERGY	http://www.broadinstitute.org/gsea/msigdb/cards/SCHLOSSER_MYC_AND_SERUM_RESPONSE_SYNERGY	32	0,6621	0,0010
Myc_RNAi_OCILy3	http://lymphochip.nih.gov/cgi-bin/signaturedb/signatureDB_DisplayGenes.cgi?signatureID=80	54	0,6451	0,0010
COLLER_MYC_TARGETS_UP	http://www.broadinstitute.org/gsea/msigdb/cards/COLLER_MYC_TARGETS_UP	25	0,6240	0,0061
MENSSEN_MYC_TARGETS	http://www.broadinstitute.org/gsea/msigdb/cards/MENSSEN_MYC_TARGETS	53	0,6022	0,0010
Myc_ChIP_PET_Expr_Up	http://lymphochip.nih.gov/cgi-bin/signaturedb/signatureDB_DisplayGenes.cgi?signatureID=245	405	0,5738	0,0010
ACOSTA_PROLIFERATION_INDEPENDENT_MYC_TARGETS_UI	http://www.broadinstitute.org/gsea/msigdb/cards/ACOSTA_PROLIFERATION_INDEPENDENT_MYC_TARGETS	84	0,5366	0,0010